



Province of British Columbia  
Ministry of Energy, Mines & Petroleum Resources  
Hon. Anne Edwards, Minister

Mineral Resources Division  
Geological Survey Branch

## GUIDE TO THE TECTONIC, STRATIGRAPHIC AND MAGMATIC SETTING OF THE MIDDLE PROTEROZOIC STRATIFORM SEDIMENT- HOSTED SULLIVAN Zn-Pb DEPOSIT, SOUTH- EASTERN BRITISH COLUMBIA

A field guide to accompany the Sullivan Project-  
Ocean Drilling Project Field Trip, Kimberley,  
B.C., 24-25 September, 1992

*Compiled by:*

Robert J. W. Turner  
Geological Survey of Canada  
100 W. Pender St. Vancouver, B.C. V6B 1R8

Trygve Höy  
British Columbia Geological Survey Branch  
Victoria, B.C.

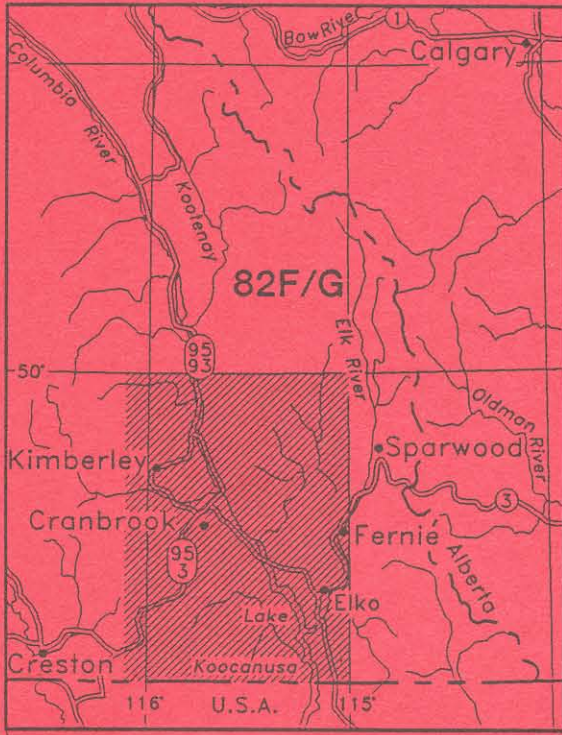
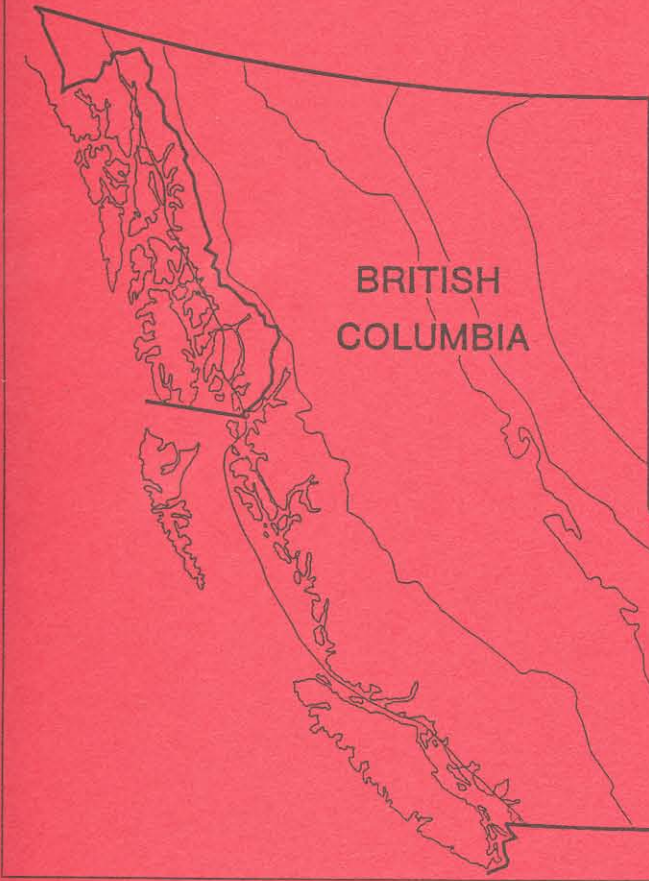
Craig H. B. Leitch  
Geological Survey of Canada  
100 W. Pender St. Vancouver  
B.C. V6B 1R8

Doug Anderson  
Cominco Ltd  
105 Industrial Rd, 2  
Cranbrook, B.C. V1C 4K7



Contribution No. 11, Sullivan-Aldridge Project  
Information Circular 1992-23

# LOCATION MAP





Province of British Columbia  
Ministry of Energy, Mines & Petroleum Resources  
Hon. Anne Edwards, Minister

Mineral Resources Division  
Geological Survey Branch

# GUIDE TO THE TECTONIC, STRATIGRAPHIC AND MAGMATIC SETTING OF THE MIDDLE PROTEROZOIC STRATIFORM SEDIMENT- HOSTED SULLIVAN Zn-Pb DEPOSIT, SOUTH- EASTERN BRITISH COLUMBIA

A field guide to accompany the Sullivan Project-  
Ocean Drilling Project Field Trip, Kimberley,  
B.C., 24-25 September, 1992

*Compiled by:*

**Robert J. W. Turner**  
Geological Survey of Canada  
100 W. Pender St. Vancouver, B.C. V6B 1R8

**Trygve Höy**  
British Columbia Geological Survey Branch  
Victoria, B.C.

**Craig H. B. Leitch**  
Geological Survey of Canada  
100 W. Pender St. Vancouver  
B.C. V6B 1R8

**Doug Anderson**  
Cominco Ltd  
105 Industrial Rd, 2  
Cranbrook, B.C. V1C 4K7



Contribution No. 11, Sullivan-Aldridge Project  
Information Circular 1992-23

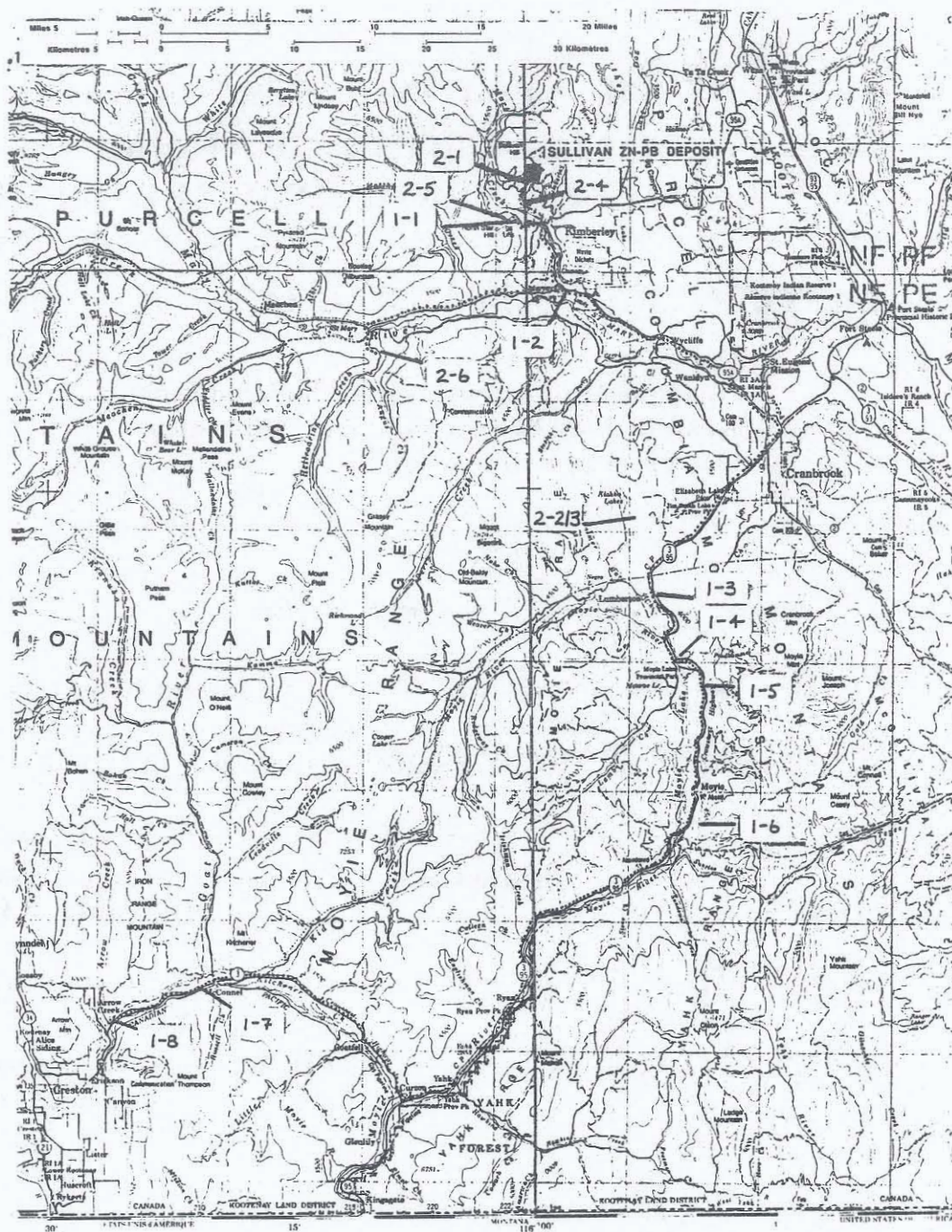


Figure 1. Route map for field trip showing locations of field stops.

# INTRODUCTION

---

The Sullivan Project - Ocean Drilling Project field trip focuses on the nature of the Aldridge Formation in the vicinity of the Sullivan mine, southeastern British Columbia. The field trip is not a general overview of the geology of this area but instead pays special attention to elucidating the tectonic setting of this Proterozoic sedimentary basin during a period of synrift turbidite sedimentation; intrusion by mafic magma; significant heating, movement and exhalation of hydrothermal fluids; and formation of extensive sediment alteration and mineralization including formation of the world class Sullivan orebody.

This field guide is a preliminary version of the guide which will be prepared for a Belt Symposium field trip in August, 1993. As such it has not been subjected to the normal scientific and editorial review process.

### The purpose of this field trip is to:

- Establish the general structural and stratigraphic setting of the Aldridge Formation (Stops 1-1, 1-2, 1-3, 1-4, 1-8);
- Demonstrate the distribution and character of the gabbro sill complex within the lower and middle Aldridge Formation (Stops 1-3, 1-6, 2-6)
- Demonstrate relationships of sediment alteration to gabbro sill contacts (Stops 1-3, 1-5, 1-6, 1-7, 2-5)
- Discuss the nature of the Sullivan stratiform zinc-lead deposit (Stop 2-1) in relation to the adjacent structural corridor of altered, mineralized and fragmented strata (Stops 2-4, 2-5).

The route of Day 1 starts in Kimberley and follows highways 95A, 95 and 3 to the vicinity of Creston (Figure 1). Day 1 focuses on stratigraphy, gabbro sills and related sediment alteration. During the morning of Day 2 the field trip will divide into two groups; one visits the Sullivan mine at Kimberley and the other, the St. Joe prospect south of Cranbrook. The

## DAY 1

STOP	PURPOSE
1-1	View, setting of Sullivan mine, North Star Ski area
1-2	Lower Aldridge Formation, Mark Creek, Marysvale
1-3	Middle Aldridge Formation and Moyie gabbro, Lumberton
1-4	marker horizon, Moyie River
1-5	Creston Formation, Moyie Fault zone
1-6	discordant pipe, middle Aldridge Formation, Moyie Lake
1-7	gabbro sill, granophyre and fragmental, Kitchener
1-8	albitite alteration, middle Aldridge Formation, N. Goat River Road

## DAY 2

STOP	PURPOSE
<i>Trip 2A</i>	
2-1	Sullivan mine tour
<i>Trip 2B</i>	
2-2	St. Joe prospect, volcanic tuff and channel deposit, Middle Aldridge Fm.
2-3	St. Joe prospect, discordant breccias, tourmalinite in Middle Aldridge Fm.
2-4	Sullivan-North Star corridor, view stop, Sullivan mine road
2-5	alteration and fragmentals, North Star Hill
2-6	view of gabbro sill-sediment stratigraphy, Bootleg Mtn., St. Mary Valley

field trip will rejoin for lunch. During the afternoon, the field trip route will start in Kimberley and continue to the southwest up the St. Mary valley. During Day 2 emphasis is placed on Proterozoic hydrothermal mineralization and alteration within the Aldridge Formation.

The guidebook uses material from earlier mapping (*e.g.* Höy, 1984, Höy and Diakow, 1982; Höy and Carter, 1988) and field trips (*e.g.* Höy *et al.*, 1985). New data and ideas come from recent reports of the B.C. Geological Survey Branch (*e.g.* Höy, 1989; in press) and Geological Survey of Canada (*e.g.* Leitch, 1991, 1992a, 1992b; Leitch *et al.*, 1991; Leitch and Turner, 1991, 1992; Turner and Leitch, 1992).

## Acknowledgments

We thank Cominco Ltd for allowing us to use of a number of unpublished reports. Of particular note are studies of the Sullivan-North Star corridor (Art Hagen, 1985) and of fragmental rocks in the Sullivan mine by Gary Delaney and Bob Hauser (1983) which were of great value. Much of this present field trip follows an informal field trip led by Doug Anderson, Cominco Ltd. and Trygve Höy in June 1991. John Hamilton provided us with useful references on many aspects, including extensive organic laminites in the modern Black Sea. Discussions with Norris del bel Belluz, John Hamilton, Marcia Knapp and Paul Ransom of Cominco Ltd., and Art Hagen and Gerry Mason have assisted our understanding of Sullivan and Aldridge geology.

Many diagrams were prepared by John Armitage of the B.C. Geological Survey Branch; others, of lesser quality, by the authors! Brian Grant is thanked for his editorial efforts in producing the manuscript, and John Hamilton and Marcia Knapp, Cominco, for editorial comments.

# GENERAL GEOLOGY OF THE BELT-PURCELL BASIN

---

T. Höy, R.J.W. Turner

## Structure

The Sullivan deposit, one of the worlds largest massive sulphide deposits, occurs within a sequence of middle Proterozoic turbidites more than 3.5 km thick in southeastern British Columbia (Figure 2). It is within the Foreland Thrust and Fold belt (Monger *et al.*, 1982), characterized by shallow, easterly verging thrust faults and broad open folds.

The structure of the western part of the Foreland Thrust belt, west of the Rocky Mountain trench (Figure 2) is dominated by the Purcell anticlinorium, a generally north-plunging structure that is cored by the middle Proterozoic Purcell Supergroup and the late Proterozoic Windermere Supergroup and flanked by Paleozoic miogeoclinal rocks. The anticlinorium is allochthonous, carried eastward and onto underlying cratonic basement by generally north trending thrust faults during the Laramide orogeny in late Mesozoic and Early Tertiary time (Price, 1981). The anticlinorium is cut by prominent northeast trending faults, including the Moyie and St. Mary faults, and along its eastern edge by north trending, west-side down normal faults, such as the Gold Creek and Rocky Mountain Trench faults (Figure 2).

The northeast trending structures are within or parallel to a broad structural zone that cuts the Purcell anticlinorium, crosses the Rocky Mountain trench and extends northeastward across the Foreland Thrust belt. A conspicuous change in structural grain, from northward north of the zone to northwestward to the south, and by pronounced and fundamental changes in thickness and facies of sedimentary rocks that range in age from middle Proterozoic to early Paleozoic. These changes reflect tectonics during filling the Purcell basin.

## Stratigraphy and Proterozoic rifting

The Purcell Supergroup succession and its correlation with contiguous Belt Supergroup rocks in the Unites States is illustrated in Figure 3. It comprises dominantly turbidite deposits of the Aldridge Formation, overlain by shallow-water to locally subaerial clastic and carbonate rocks. The Nicol Creek basalts are a prominent marker succession that is centred near the present position of the Rocky Mountain trench. Within the Aldridge Formation and correlative rocks east of the trench, the Fort Steele Formation, is a thick sequence of gabbroic sills and dikes, the Moyie sills, that locally were intruded into wet, unconsolidated sediments (Höy, 1989). A U-Pb zircon age of 1445 Ma on one of these sills (Höy, *op cit.*) provides a minimum age for Aldridge sedimentation and formation of the Sullivan deposit. These sills and associated alteration will be the focus of a number of stops.

The Purcell Supergroup has been affected by several episodes of deformation in middle and late Proterozoic time. The earliest event recorded in Purcell stratigraphy is schematically shown in Figure 4. It comprised extensional tectonics resulting in prominent block faulting along the margin of the Purcell basin during deposition of the Fort Steele and Aldridge formations. The Boulder Creek fault and the segment of the Rocky Mountain trench fault north of Boulder Creek coincide with a marked change in the character of lower Purcell rocks, from dominantly fluvial (Fort Steele Formation), shallow-water and minor turbidite deposits in the Northern Hughes Range to a thick succession of Aldridge turbidites west of the trench. In late middle Aldridge time, turbidite deposition extended over the basin margin (Figures 4b, 5); evidence of growth faulting is not evident in late Aldridge time as upper Aldridge rocks extend across the basin margin.

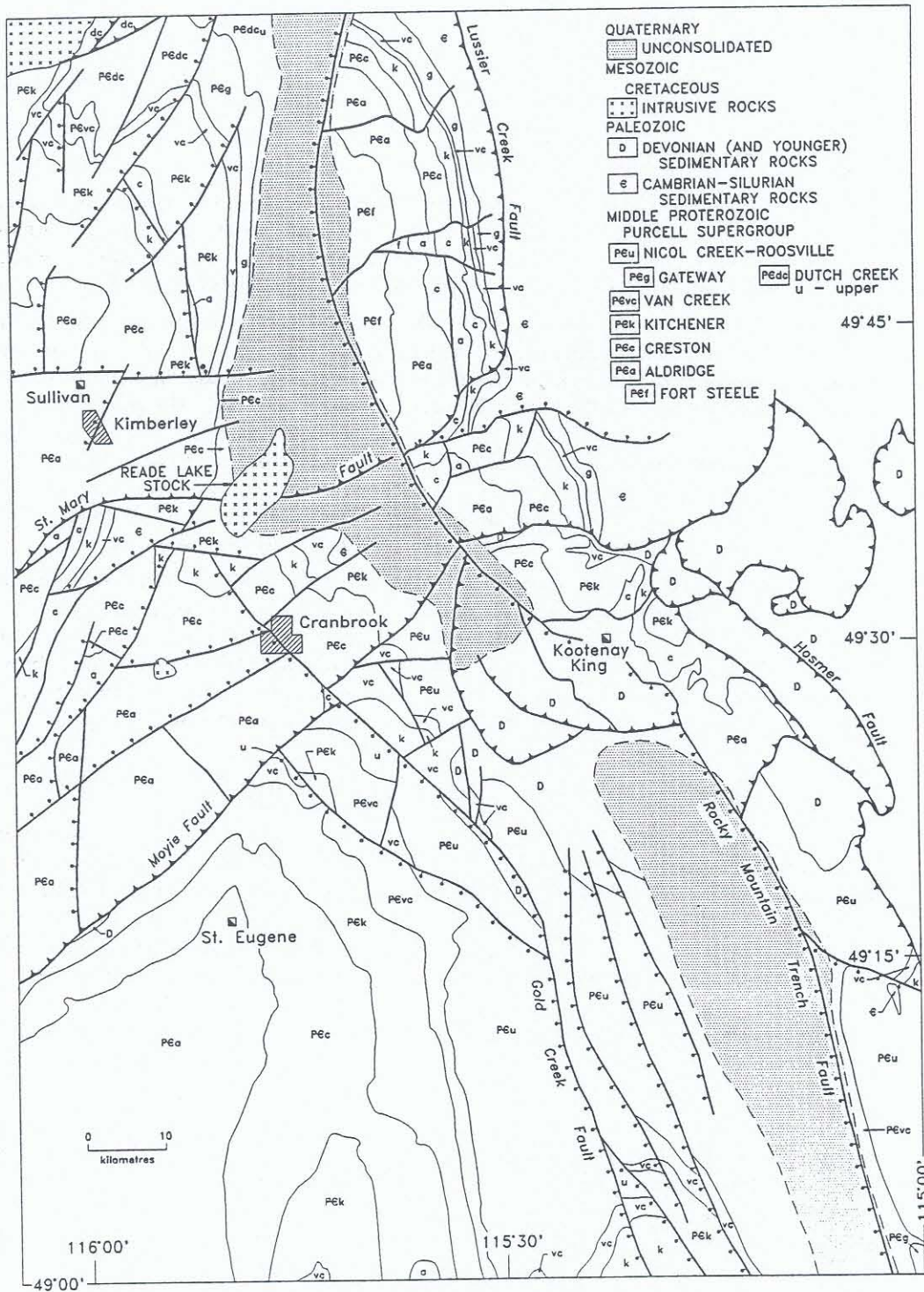


Figure 2. Geological map of the Fernie west-half map sheet and eastern part of the Nelson east-half (from Höy and Carter, 1988; Höy, in press)

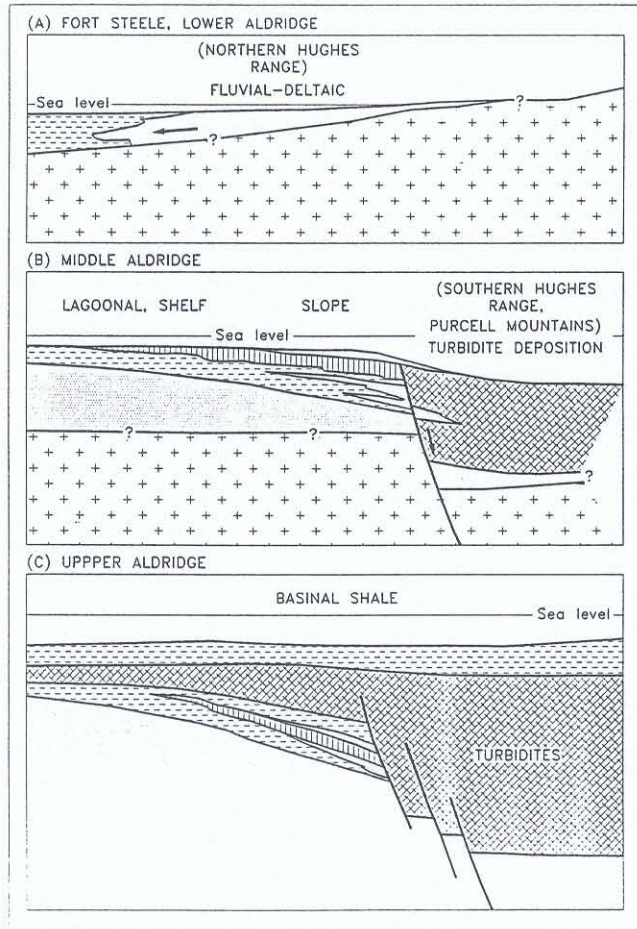


Figure 4. Tectonic evolution of the northeastern margin of the Purcell basin in Fort Steele and Aldridge times (from Höy, in press).

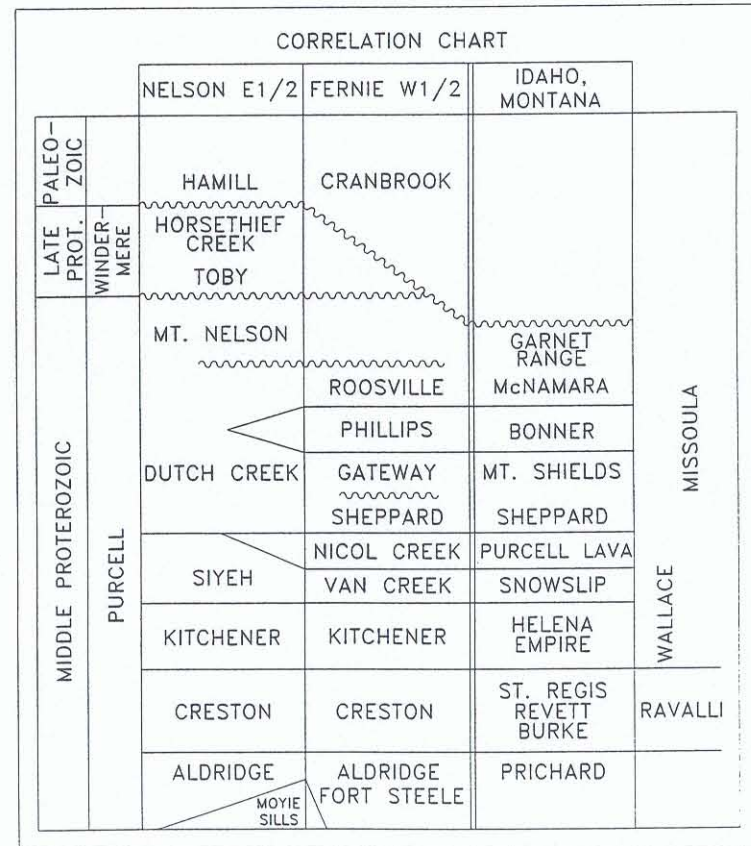


Figure 3. Table of formations, Purcell Supergroup, and correlation with Belt Supergroup

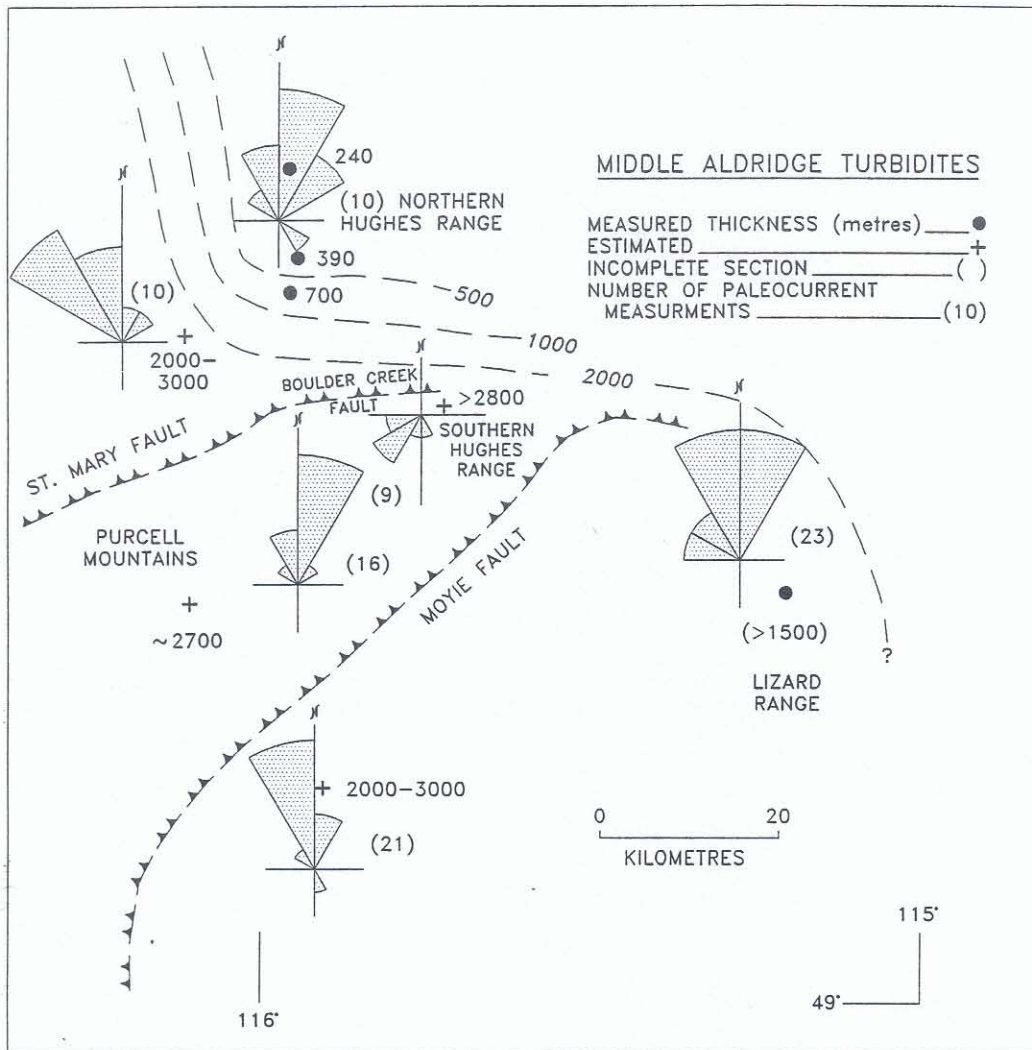


Figure 5. An isopach map of middle Aldridge turbidites, restored for movements on the St. Mary and Moyie faults. Rose diagrams are measured and restored paleocurrent directions from basal scours and cross laminations (from Höy, in press).

Tectonism continued along the Purcell basin margin during deposition of younger Purcell Supergroup rocks. An isopach map of the Nicol Creek Formation shows that the most voluminous extrusion of basaltic lava occurred along the eastern margin of the basin (Höy, in press). In the Skookumchuck area 30 kilometres northeast of Sullivan, dramatic changes in thickness and facies of the Sheppard and Gateway formations are caused by extensional growth faults and resultant subsidence (Figure 6). The overlying Phillips Formation, a regional mauve-coloured marker unit in both Belt and Purcell supergroup rocks, also dies out here, supplanted to the north by green facies in the Dutch Creek Formation.

Tectonic instability along the Purcell basin margin is also evident in the Moyie Lake area southeast of Cranbrook. A prominent fluvial conglomerate, up to 9 metres thick, has locally cut through and removed up to several hundred metres of the Nicol Creek Formation (Höy, in press). Clasts within the conglomerate include some medium-grained intrusive boulders that have been dated at *ca.* 1514 Ma. The size of these boulders and their inferred exotic provenance suggests that basement must have been exposed locally during deposition of late Purcell Supergroup rocks. This implies development of growth faulting with consid-

erable movement as the boulder conglomerate is underlain by at least 9 kilometres of Purcell Supergroup stratigraphy.

In summary, the Purcell Supergroup in the Sullivan area was deposited along a tectonically active basin margin. Dramatic thickness and facies variations here record Purcell-age growth faults and contrast with gradual changes characteristic of most Purcell and Belt rocks elsewhere. These faults reflect deep crustal structures, structures that modified incipient Purcell rifting, and led to the development of an intracratonic basin in middle Proterozoic time.

## Paleogeographic setting

Recent paleotectonic reconstructions of the Proterozoic supercontinent (*e.g.* Hoffman, 1991) would suggest an intracratonic position of the Belt-Purcell basin (Figure 7). This strengthens arguments that the Belt-Purcell basin formed below an intracratonic lake (Winston, 1984), possibly analogous to the rift setting of Lake Baikal, Russia or the East African Rift system. If a marine environment, the Belt-basin was part of an elongate, narrow seaway, perhaps analogous to parts of the Gulf of California or the Red Sea. In either case, the Belt Basin lay within a large landmass. Paleomagnetic data that suggest an equatorial latitude and the fact the Proterozoic continents were unvegetated suggest a lake or marine basin in a hot desert landscape. North to south turbidite paleocurrent data from the Aldridge Formation suggest sediment input, likely fluvial, from the south. It would also be expected that aeolian sedimentation within the basin could have been significant (*See Stop 1-4*).

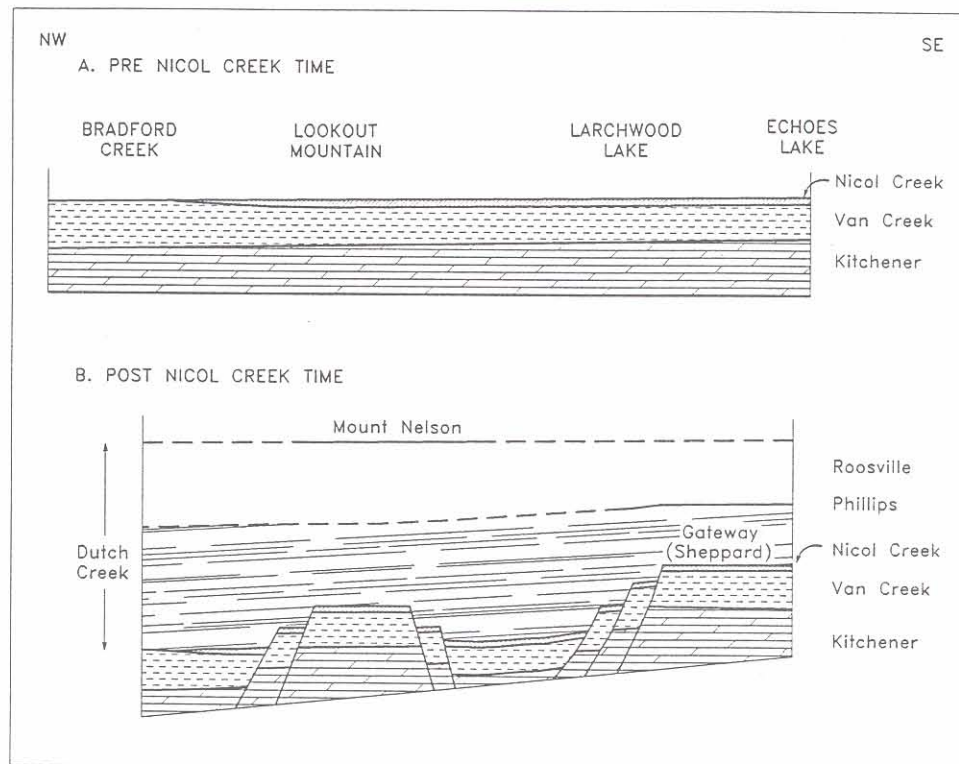


Figure 6. Postulated model for deposition of upper Purcell rocks, Skookunchuck area, showing effects of late Purcell tectonism (after Carter and Höy, 1987).

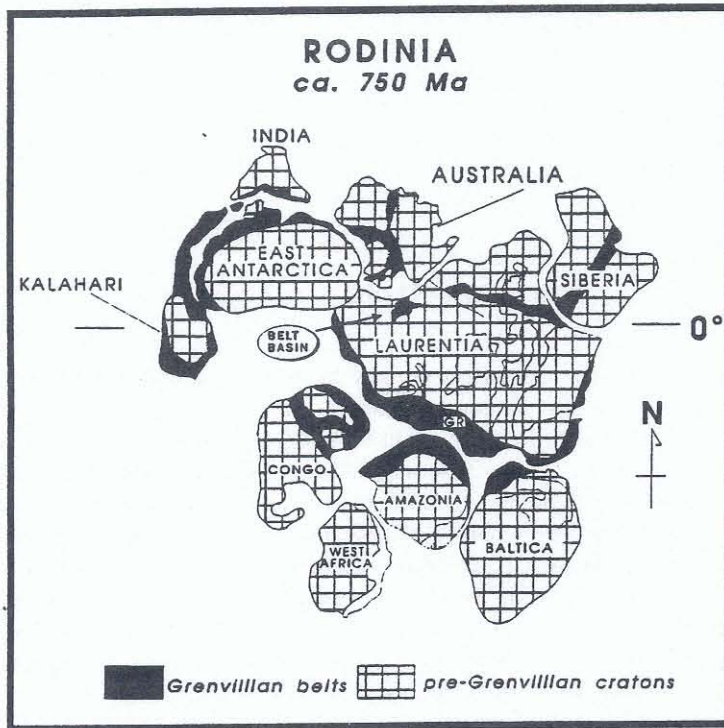


Figure 7. Paleotectonic reconstruction of Proterozoic supercontinent. Location of Belt-Purcell basin is noted (from Ross, 1992).

## FIELD TRIP ROAD LOG AND COMMENTS

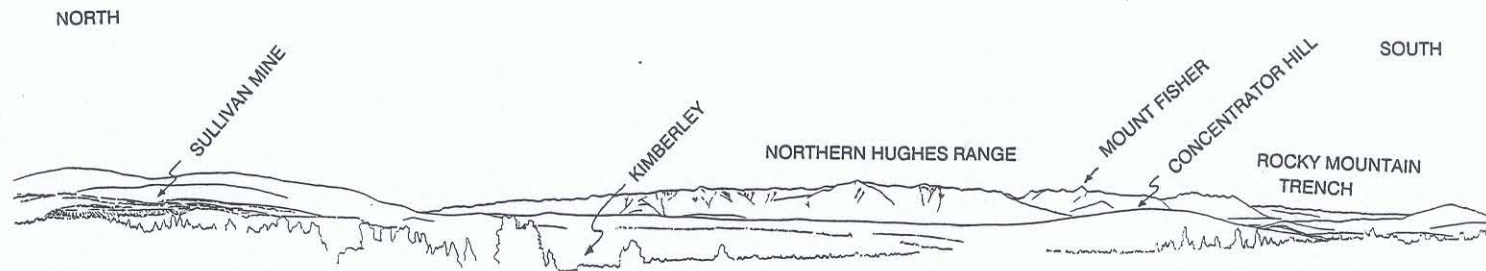


Figure 8. Panoramic view from base of Kimberley Ski area (Stop 1-1) looking from northeast to southeast. Visible are the Sullivan mine, St. Marys River valley, the Rocky Mountain Trench, and the Hughes Range and Steeples east of the Rocky Mountain Trench. Approximate locations of the Kimberley fault, St. Marys fault, Rocky Mountain Trench fault, as well as distribution of rock units.

# DAY 1: KIMBERLEY TO CRESTON: STRATIGRAPHY, GABBRO SILLS AND ALTERATION

---

The ODP-Sullivan field trip starts at the Purcell Condominium, Kimberley Ski Resort, Kimberley. For the convenience of future guidebook users all distances are given from the traffic lights at Ross and Wallinger Streets, the main intersection in downtown Kimberley.

## Start Point

---

**0.0 km** Ross St. and Wallinger St., Kimberley, B.C. Drive west on Ross St. (which becomes Gerry Sorenson Way) following signs to Kimberley Ski Area. Ascend switch backs passing Happy Hans Campground. Stay left at fork in road to Purcell, Rocky Mountain and Silver Birch Condominium/chalets. Turn right at top of hill onto road to ski lodge complex; pull off on right side (Figure 1).

## STOP 1-1:

---

### *VIEW OF SULLIVAN MINE AND ENVIRONS, NORTH STAR SKI AREA (Höy)*

This stop provides an overview and introduction to the regional geological setting of the Aldridge Formation and the Sullivan deposit. The comments below are largely summarized from the previous general geology section.

The view (Figure 8) looks across the Rocky Mountain trench to the Hughes Range in the Western Rocky Mountains. In the foreground, along the eastern edge of the Purcell Mountains, is the Sullivan mine and Concentrator Hill across which occurs the lower-middle Aldridge contact and the stratigraphic position of the Sullivan deposit. In the distance, Fort Steele Formation rocks are exposed on the lower slopes of the Hughes Range, overlain by the Aldridge Formation and younger Purcell Supergroup rocks.

## Comment

The Rocky Mountain Trench coincides, at this latitude, with a west-side down Tertiary normal fault, the Rocky Mountain Trench fault. It follows approximately the locus of prominent facies and thickness changes in middle Proterozoic Purcell rocks, with fluvial quartzites of the Fort Steele Formation at the base of the succession in the Northern Hughes Range and correlative deep-water turbidite facies in the Purcell Mountains.

The Boulder Creek fault, which occurs in the valley just north of Mount Fisher (Figure 8), also follows the locus of a middle Proterozoic structure. To the south, turbidites similar to those in the Purcell Mountains are exposed. Thus the Boulder Creek fault and a segment of the Rocky Mountain trench fault outline a block of Purcell rocks in the Northern Hughes Range that marks the northern and eastern edge of the Purcell basin.

Return to Kimberley.

**0.0 km** Ross St. and Wallinger St., Kimberley, B.C. Drive south on Wallinger (Highway 95A).

**5.8 km** Intersection, St. Marys Lake Road; continue on 95A.

## STOP 1-2

### 6.6 km LOWER ALDRIDGE FORMATION, MARK CREEK, MARYSVILLE (Höy and Anderson)

As you enter Marysville, park on north side of road immediately east of bridge across Mark Creek (Figure 1). Cross road and footbridge to boardwalk trail along west side of creek.

The lower Aldridge Formation, comprising thin-bedded, well-laminated argillite and wacke is well exposed in the walls of the creek, especially downstream from the falls.

### Comment

The lower Aldridge comprises dominantly rusty-weathering, thin to medium-bedded, fine-grained quartz wacke and siltstone. Quartz wacke beds are commonly graded or locally crossbedded and, less commonly, have well-developed basal scours indicative of turbidite deposition. In the Kimberley area, a succession of grey-weathering quartz wacke and arenite 250 metres thick ("lower quartzite") occurs approximately 300 metres below the Sullivan horizon and the base of the middle Aldridge. The contact with the middle Aldridge is placed at the base of the first prominent blocky, grey-weathering quartz wacke bed. The contact is generally gradational and rusty-weathering quartz wacke beds are conspicuous in the top few tens of metres of the lower Aldridge. To the southwest east of Creston (*see* Figure 1), the distinction between the upper part of the lower and the middle Aldridge is less pronounced and it is difficult, based on lithology alone, to separate them.

The average modal composition of "unaltered" lower Aldridge siltstones based on six samples (*see* Fig. 28) is: quartz 40%, biotite 30%, muscovite 10%, K-feldspar 10%, plagioclase 7%, sphene 3%, tourmaline 2%, pyrite 2%, organic carbon 1%, pyrrhotite 1%, and trace amounts of chlorite, carbonate, epidote, monazite, apatite, rutile, and ?zircon. These modal data compare reasonably well with data of Edmunds (1977), who found evidence of a bimodal population amongst his 95 samples of dominantly middle Aldridge rocks, leading him to classify them into "argillite" and "greywacke".

Based on their common occurrence as anhedral grains with a clast-like habit, we interpret the quartz, plagioclase, apatite, monazite and possibly some of the coarse muscovite to represent original detrital components. Albitization of K-feldspar and plagioclase, common below 2500 m depth during sediment diagenesis (Boles, 1982), and metamorphism, account for the albitic feldspar; biotite is interpreted as metamorphosed detrital and authigenic clays. Tourmaline, characterized by coarse (0.1 - 0.2 mm) euhedral schorl (iron tourmaline), may be of detrital or diagenetic origin. Epidote replaces some plagioclase and may be related to the diagenesis or metamorphism of feldspars. Sphene appears detrital in unaltered sediments but can also occur as part of the hydrothermal assemblage. Apatite may be detrital or metamorphic after an authigenic phosphatic mineral. Pyrrhotite and pyrite are common minerals, presumably related to diagenetic sulphate reduction in shallowly buried sediments.

### 6.7 km Marysville

**12.9 km** Hill to west (Lone Pine Hill) is underlain by irregular bodies of gabbro (Höy and Carter, 1988).

**15.3 km** Junction, Wycliffe Road

**15.9 km** View across St. Marys River. Bluffs on south side expose Pliocene gravels and sands.

**21 km** Bridge over St. Marys River

**26.2 km** Railway overpass

**28.3 km** Junction of Highways 95A and 95/3. Take onramp onto Highway 95/3 heading south. Drive through Cranbrook following signs for Highway 95/3 (at second lights turn right).

37.4 km Travel Information Center (east side) and Jim Smith Road (west side).

42.4 km bluffs to west expose gabbro (Höy and Carter, 1988).

### STOP 1-3

#### 48.4 km: *MIDDLE ALDRIDGE FORMATION AND MOYIE SILL-ALDRIDGE CONTACT, LUMBERTON ROAD TURNOFF (Höy)*

Pull off on west side of Highway 95/3 at junction with Lumberton Road (Figure 1). Low cliffs on east side of highway expose middle Aldridge strata. A trail at the south end of the roadcut heads east from the road and upslope to the base of the cliffs that are visible from the highway. At the base of the cliff is a contact between gabbro (cliff-former) and underlying strata.

### Comment: Middle Aldridge Formation

The middle Aldridge comprises 2000 to 3000 metres of dominantly well-bedded, medium to locally coarse-grained quartz arenite, wacke and siltstone. In general, the basal part comprises interbedded quartz wacke and arenite with only minor sections of silty argillite. Within the upper part, beds are typically thinner and the proportion of siltstone and argillite increases. The upper part of the middle Aldridge comprises a number of distinct cycles of massive, grey arenite beds that grade upward into an interlayered sequence of wacke, siltstone and argillite, and are capped by siltstone and argillite.

Arenite and wacke beds of the middle Aldridge have many structures typical of classical turbidite deposits, and many of these are well displayed at this road exposure. Beds are laterally extensive and commonly parallel sided. Some may have internal stratification, with graded, laminated and crosslaminated divisions. Only rarely, however, is the ideal Bouma facies represented. Sole markings, including scours and tool marks, indicate a generally northward current transport direction (Figure 5). Within the finer grained turbidites, convolute laminations, ripple bedding, and flame structures occur. Concretionary bodies and rip-up clasts occur in some beds, and large crystal casts with the swallow tail form of selenite are found in some of the more argillaceous beds.

### Moyie Sill - Aldridge Formation Contact

On the cliffs above the middle Aldridge turbidite exposure is a gabbro sill 66 metres thick. It is approximately 1000 metres above the base of the middle Aldridge and is one of a number of similar sills within the lower Aldridge and lower part of the middle Aldridge. This stop allows a detailed look at the base of one of these sills, the Lumberton sill, and its contact with the Aldridge Formation.

A schematic section of the Lumberton sill is shown in Figure 9. It is cut by vertical quartz-carbonate-sulphide veins with wide hydrothermally altered selvages. Its contact with the Aldridge Formation, illustrated in Figure 10, is sharp. Buff-coloured, fine-grained siltstone (Unit a) with abundant fine aligned muscovite is overlain by coarser grained, granular quartz wacke (Unit b). Evidence of alteration includes abundant biotite, dispersed epidote and calcite and large isolated chlorite grains. Unit c, immediately adjacent to the sill (Figure 10), comprises dominantly fine-grained granular albite (?) with minor dispersed epidote and ragged grains of biotite. The contact phase of the sill (Unit d) is intensely altered with large, irregular poikilitic grains of hornblende and abundant chlorite and biotite crystals in a fine-grained matrix of plagioclase (albite?), quartz, epidote, biotite and calcite. This alteration, including biotite, albite and hydrothermal minerals, is typical of contact sill alteration. Stops 6 and 7 will also examine alteration and structures associated with emplacement of other Moyie sills.

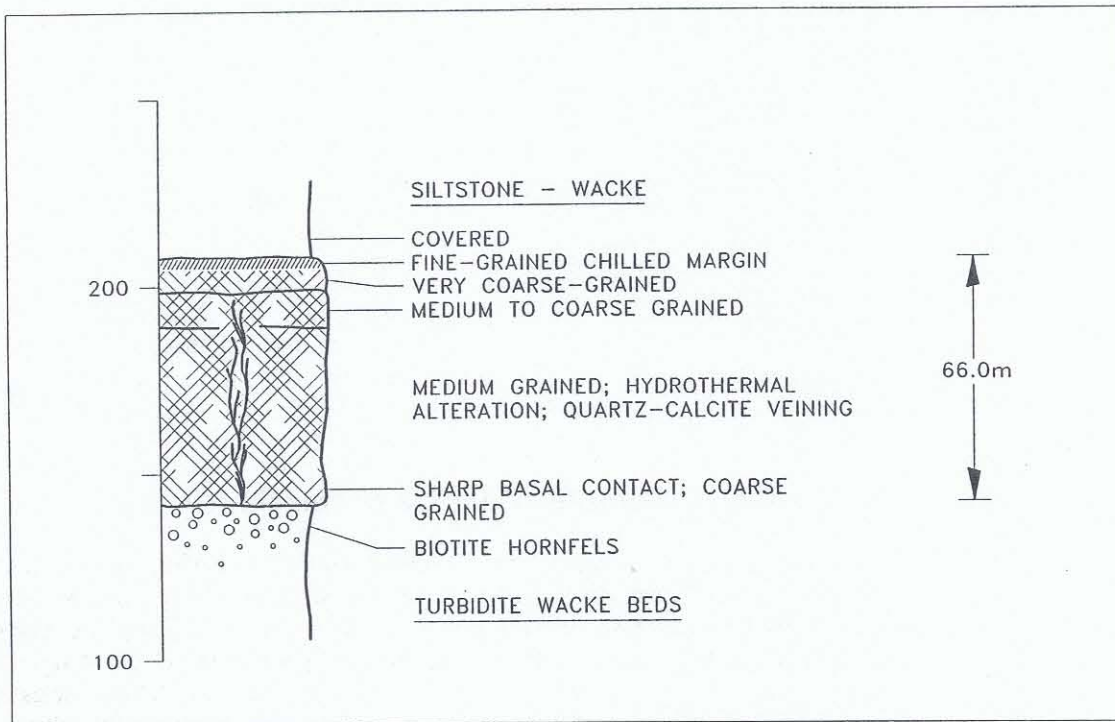


Figure 9. A section through the Lumberton sill, located 10 kilometres due north of Moyie Lake, showing coarse hornblende at the base of the sill and cross-cutting veins (Stop 1-4).

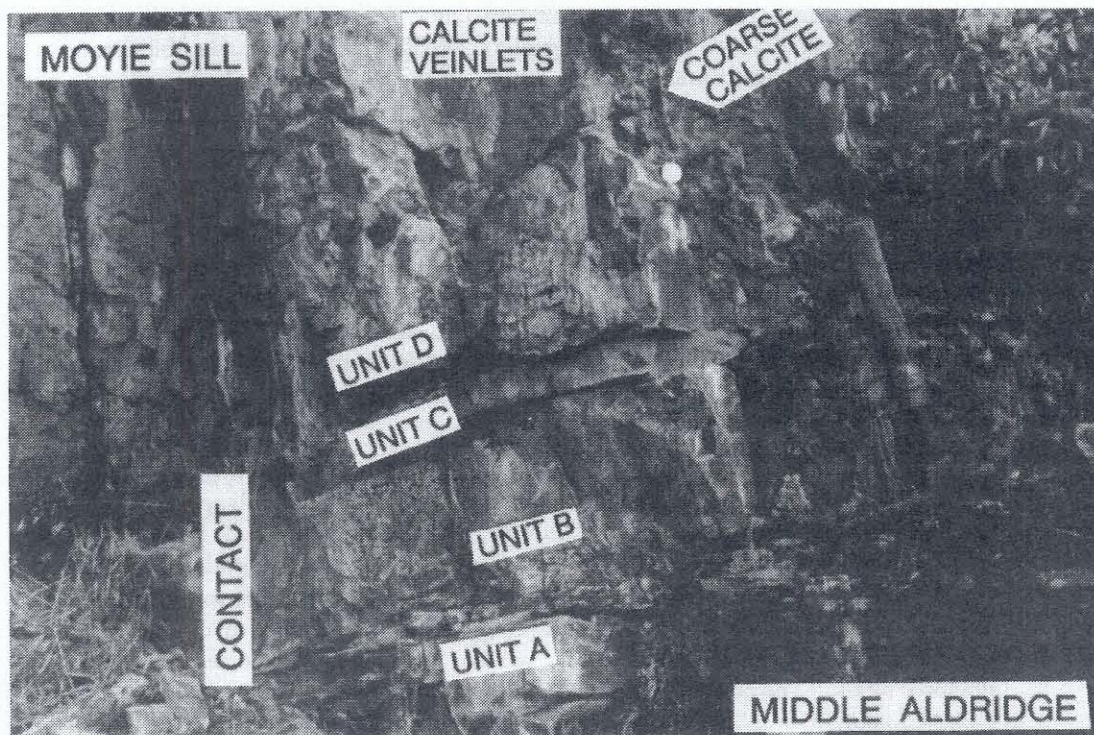


Figure 10. Photograph of basal contact of sill with underlying sediments (Stop 1-4).

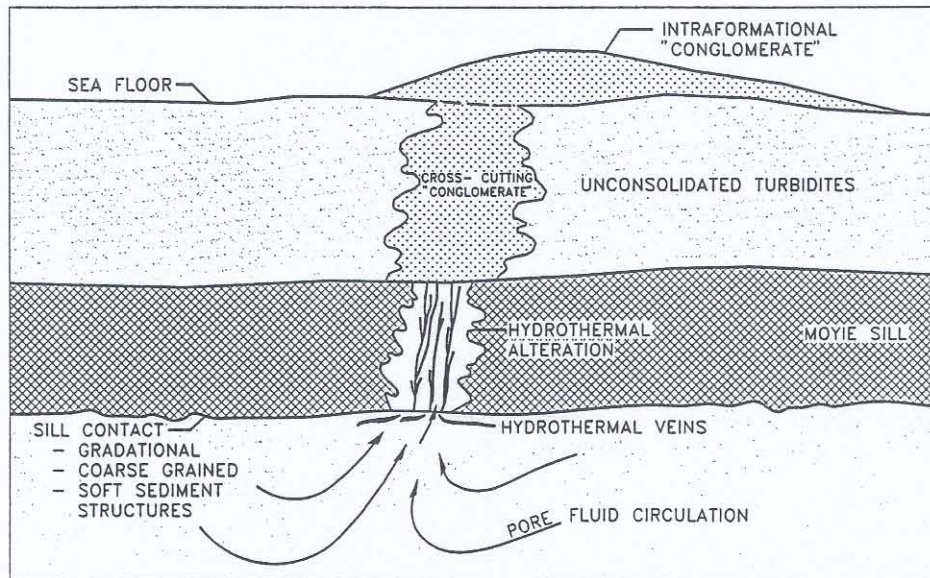


Figure 11. Model for injection of a Moyie sill into unconsolidated middle Aldridge turbidites (from Höy, 1988).

### Comment

The Moyie sills comprise dominantly relict hornblende and plagioclase phenocrysts in a matrix of altered plagioclase, hornblende, quartz, chlorite and epidote. They are typically subalkaline, low-potassium, high-iron tholeiites. Locally, however, Moyie sills are alkali basaltic in composition (Höy, 1989).

A number of Moyie sills have unusual contacts and internal structures that indicate that they intruded unconsolidated wet sediments (*see* model, Figure 11). These include gradational contacts between sills and sediments, structures attributed to soft sediment deformation, obliteration of sedimentary structures immediately adjacent to sills, and large-scale dewatering structures (Höy, 1989; *in press*).

52.2 km gabbro, road cut

54.9 km bridge, Moyie River

### STOP 1-4

#### 54.9 km MARKER LAMINAE, MOYIE RIVER BRIDGE (Turner and Leitch)

Pull off on west side of Highway 95/3 immediately south of bridge (Figure 1). Cross to east side of highway. Climb fence (be careful not to damage fence) and walk to base of cliff exposing middle Aldridge strata. Packets of marker laminae occur interbedded with turbidite and argillite beds.

These marker laminae are composed of quartz-biotite-feldspar-epidote-tourmaline-sphene-allanite-carbon, typical of middle Aldridge strata (Leitch *et al.*, 1991). Dark laminae differ from lighter laminae only by a greater abundance of epidote, sphene, allanite and organic carbon yielding a distinctive Ca-Ti-C-REE geochemical signature.

## Comment

Laminated marker units have been recognized throughout the stratigraphic thickness of the middle Aldridge Formation. Recognition and correlation of marker units has resulted from the work of Cominco Ltd. over the last 25 years. In particular, detailed knowledge of the characteristics of these markers has resulted from the work of Art Hagen. Each marker unit has a unique sequence of light and dark laminae couplets that have been correlated over distances of several hundred kilometres (Heubschman, 1973).

Turbidite beds are variably interbedded within a laminitic package, locally thickening the marker unit. Turbidite lobes within the middle Aldridge Formation, correlated using marker units and offset by the Kimberley Fault, have been used to assist in the determination of net movement on the fault and thereby enable testing for the offset position of the Sullivan orebody. To date, the sediment/intrusive package indicative of the Sullivan sub-basin, with some Pb-Zn sulphides, has been intersected at depth (Hagen *et al.*, 1989).

Both dark and light laminae are composed of quartz-feldspar-muscovite-biotite silt, similar in composition to silts throughout the middle Aldridge Formation. Petrographically, the pale laminae are similar in composition to dark laminae except for greater organic content, allanite and sphene (Heubschman, 1973; Leitch *et al.*, 1991).

What component of the laminitic (*i.e.* dark laminae or light laminae) reflects ambient sedimentation and what reflects episodic sedimentation is an unresolved issue of significant importance to the interpretation of the origin of the laminites. Reconnaissance inspection of marker laminae units throughout the middle Aldridge Formation reveal that the boundaries between pale and dark laminae are typically diffuse, but occasionally the base of pale laminae are sharp. Such asymmetric beds with sharp bases and gradational tops suggest rapid sedimentation of pale detrital silt interrupted the ambient dark more organic-rich sedimentation.

Heubschman (1973) interpreted the dark laminae as the fallout of organic blooms in surface waters above a stagnant watermass. Recent work in the Black Sea recognizes laminites that correlate over distances in excess of 1000 km; laminites are composed of alternating white coccolithophorid laminae and black terrigenous laminae (Hay and Honjo, (1989). Spring planktonic blooms in surface waters form white laminae; terrigenous sedimentation appears to be ambient. This model suggests that the dark organic laminae are episodic; it is unclear how this model might explain the asymmetric nature of pale laminae.

An alternate hypothesis for the origin of the marker laminites in the Aldridge basin involves episodic sedimentation of terrigenous material from dust storms. Such aeolian deposits could be very widespread if caused by major seasonal storms and would interrupt ambient, more organic sedimentation. Laminites in the Gulf of California that have been correlated throughout a 20 kilometre study area are composed of alternating diatomaceous and terrigenous laminae (Baumgartner *et al.*, 1991). Terrigenous laminae are interpreted as aeolian rather than river-derived sediments as the lamina sequence does not correspond to the discharge data for nearby rivers (Baumgartner *et al.*, 1991). Material transport is associated largely with summer convective thunderstorms. The setting of the Aldridge lake/sea as an intracontinental waterbody at equatorial latitudes surrounded by vast desert continents would suggest that some form of aeolian sedimentation occurred.

**56.8 km:** Moyie Fault zone. The Moyie fault zone underlies this valley bottom. (*see* Stop 1-5).

**57.3 km:** Roadcuts of Kitchener Formation.

## STOP 1-5

---

**58.1 km:** *CRESTON FORMATION, MOYIE FAULT SYSTEM, MOYIE LAKE*  
(Höy)

Park in pullout on west side of highway at curve to east (Figure 1). The pullout has an excellent view south and west down and across Moyie Lake. Roadcuts on the east side of the highway expose Creston Formation. This stop provides a look at the shallow-water succession that overlies turbidites of the Aldridge Formation and an overview of the Moyie fault system, one of the northeast-trending faults with a history of movement that can be traced back to the Proterozoic.

## Creston Formation

Roadcuts on the east side of the highway expose rocks of the Creston Formation. The Creston Formation is at the base of succession greater than 5 kilometres thick of shallow water and subaerial clastic, carbonate and volcanic rocks. The Creston Formation represents the shoaling of the Aldridge lake/sea to a shallow-water/subaerial environment. It comprises three main subdivisions: a basal silty succession of thin-bedded grey to green siltstone and argillite, a middle quartzite succession of coarser grained siltstone and quartz arenite, and an upper succession of intermixed green argillaceous siltstone and minor quartz arenite. This stop, near the top of the middle member of the Creston Formation, shows many of the sedimentary structures indicative of shallow-water deposition: desiccation and syneresis cracks, mud-chip-breccias, scour-and-fill structures, ripple marks, crossbedding and graded bedding. The characteristic bed-form is thin bedded, wavy, commonly laminated argillite-siltite couplets.

## Moyie Fault, Proterozoic And Paleozoic Tectonics

The Moyie Lake view is dominated by a thick succession of northeast dipping Creston Formation rocks on the west limb of the Moyie anticline. The Moyie fault is well exposed in the valley to the west. In the far distance on the east side of the lake, workings of the St. Eugene deposit are visible. The deposit occurs in middle and upper Aldridge rocks in the core of the Moyie anticline.

## Comment

The Moyie fault and its extension east of the Rocky Mountain trench, the Dibble Creek fault, is a right-lateral reverse fault with an estimated displacement of 12 kilometres during eastward thrusting in the late Mesozoic (Benvenuto and Price, 1979; Figure 2). It follows the locus of an earlier structure, documented by prominent facies changes in lower Paleozoic rocks.

North of the Moyie fault, a sub-Cambrian unconformity truncates Windermere and Purcell rocks at a slight angle, indicative of tilting prior to deposition of Cambrian rocks. A tectonic high, referred to as "Montania" (Deiss, 1941), occurred south of the fault in pre-Devonian time. North of the Moyie-Dibble faults, a thick sequence of Cambrian through Silurian beds is exposed; to the south, Devonian rocks unconformably overlie upper Purcell rocks (see Figure 3).

A parallel fault, the St. Mary fault and east of the Rocky Mountain trench, the Boulder Creek fault, has documented movement in middle Proterozoic time during deposition of the Aldridge and Fort Steele formations (see Stop 1; Höy, 1982; 1984). In late Proterozoic time, the St. Mary fault was also the locus of extensional block faulting (Lis and Price, 1976), referred to as the Goat River orogeny (McMechan and Price, 1982). Northwest of the fault, an increasingly thicker succession of Windermere rocks is exposed beneath a lower Cambrian unconformity as the fault is approached. Farther southwest, at the south end of Kootenay Lake, the Windermere is more than 9 kilometres thick and includes a number of conglomerate units that contain clasts derived locally from the underlying Purcell Supergroup. South of the St. Mary fault, the Windermere is absent and the Cambrian unconformity cuts Purcell rocks.

These northeast-trending structures have important implications for base metal deposits. They parallel crustal structures, recognized by prominent magnetic lineations and a gravity low (Kanasewich, 1968), which locally controlled the configuration of the Purcell basin

margin and localized structures that may have controlled the discharge of metalliferous fluids that led to the formation of stratiform sulphide deposits.

67.1 km: Village of Moyie

67.5 km: dumps, St. Eugene Mine

## STOP 1-6

---

### 69.6 km: *DISCORDANT PIPE, MIDDLE ALDRIDGE FORMATION, MOYIE LAKE (Turner, Leitch and Anderson)*

Pull off on west side of Highway 3 just south of guard rail at 70.1 km (Figure 1). Walk north 0.5 km to bold road cuts on east side of highway. A pipe-like zone of massive unbedded sandy siltstone cuts across a bedded sequence of turbidite silts and sands in the upper part of the middle Aldridge Formation (Figure 12). On the north side of the pipe the steeply dipping contact is sharp but very irregular and locally follows bedding contacts. This irregular contact suggests formation prior to lithification of the sediment. Within the pipe the sandy silt is very homogenous, lacks any evidence of bedding, and locally contains fragments of siltstone and mudstone to 1 cm. The contact on the south side of the pipe is more diffuse and cuts bedding at a shallow angle near road level. The sediments within the pipe appear to have been fluidized and transported a distance sufficient to obscure bedding.

### Comment

It is possible that the pipe structure fed a silt/sand volcano that erupted on the floor of the Aldridge lake/sea although such bedded units have not been recognized above the Moyie pipe. A thick unit of massive siltstone to fine sand wacke ("granule wacke") occurs extensively within the Sullivan-North Star trend (Stops 2-5 and 6) and this unit is interpreted to have erupted from a series of underlying pipes similar to the Moyie pipe.

100.3 km: bridge over Moyie River, north end of village of Yahk

104.7 km: Junction with Highway 3. Turn right (east) on Highway 3.



Figure 12. Sketch from photograph of Moyie discordant pipe exposed in roadcut near Moyie Lake (Stop 1-6). View looking south from west side of road just north of pipe. Extent of massive and locally fragmental rock of pipe shown in stipple pattern.

**111.0 km:** GOATFELL TOURMALINITE OCCURRENCE. Prominent knob that rises above railway track several hundred meters south of highway is a tourmalinite body in the middle Aldridge Formation.

**123.8 km:** Village of Kitchener

## STOP 1-7

### **125.3 km: MOYIE SILL, ALTERED AND FRAGMENTED ALDRIDGE FORMATION, KITCHENER (Höy and Anderson)**

Pull off on north side of Highway 3, opposite 5-10 m high roadcuts on south side of highway that extend from mileage 125.2 to 125.7 km (Figure 1). A sill complex, comprising two gabbroic sills with an intervening section of altered and brecciated middle Aldridge quartzite is exposed near the northeast end of the roadcuts. The sill complex and associated brecciation at or near the top has been traced at least 3 kilometres (D. Anderson, personal communication, 1991). It contrasts with the basal sill contact at Stop 3 and the soft-sediment features described by Höy (1989) in a lower Aldridge sill at Lamb Creek west of Moyie Lake.

The contact of the Aldridge metasediments with the upper sill is sharp (Figure 13). The metasediment-lower sill contact is not exposed; the lower sill outcrops approximately 130 metres to the southwest along Highway 3.

Only the top few metres of the metasediment unit are exposed. It comprises altered biotitic quartzite (biotite hornfelsed quartzite/granophyre) overlain by a matrix-supported fragmental with of boulder-sized clasts. Lack of primary sedimentary structures, including bedding planes, in the altered quartzite suggests homogenization of a sediment. The quartzite comprises dominantly recrystallized quartz and minor saussuritized feldspar grains overgrown with abundant biotite and minor plagioclase (albite?). Disseminated epidote, minor chlorite and variable amounts of calcite indicate hydrothermal overprinting. The top of the metasediment unit (Plate 4) contains an increasingly larger proportion of rounded quartzite cobbles and boulders floating in a granular quartzitic groundmass. Their similarity in composition to the groundmass, roundness, diffuse boundaries and matrix support suggests disaggregation of a partly consolidated sediment.

**129.7 km:** bridge, Goat River

**133.0 km:** Junction with Arrow Creek East Road. Turn north onto Arrow Creek East Road.

**133.4 km:** Junction with North Goat River Road. Take right fork (main paved route) onto North Goat River Road.

## STOP 1-8

### **133.7 km: ALBITITE, NORTH GOAT RIVER ROAD (Turner, Leitch and Anderson)**

Park on south (right) side of road across from prominent road cuts. The roadcut exposes a discordant white to pale grey massive albite ("albitite") alteration zone within a sandstone turbidite sequence within the middle Aldridge Formation (Figure 14). The albite alteration is most intense along a series of northeasterly-trending steeply dipping structures in the southern part of the road cut. Laterally, the massive discordant albitite interfingers to the west and east with dark green to grey chlorite-muscovite-albite altered rock. These concordant albitite zones occur in the thicker sandstone beds while chlorite-sericite-albite alteration occurs in more thin-bedded sandstone, siltstone and argillite sequences. This relationship suggests fluid flow was focused along the steep structure and spread laterally along permeable sandstone beds. Towards the north end of the road cut, the bedded turbidite sequence is biotitic and is only weakly altered. Note that these least altered sediments are distinctly iron stained (typical

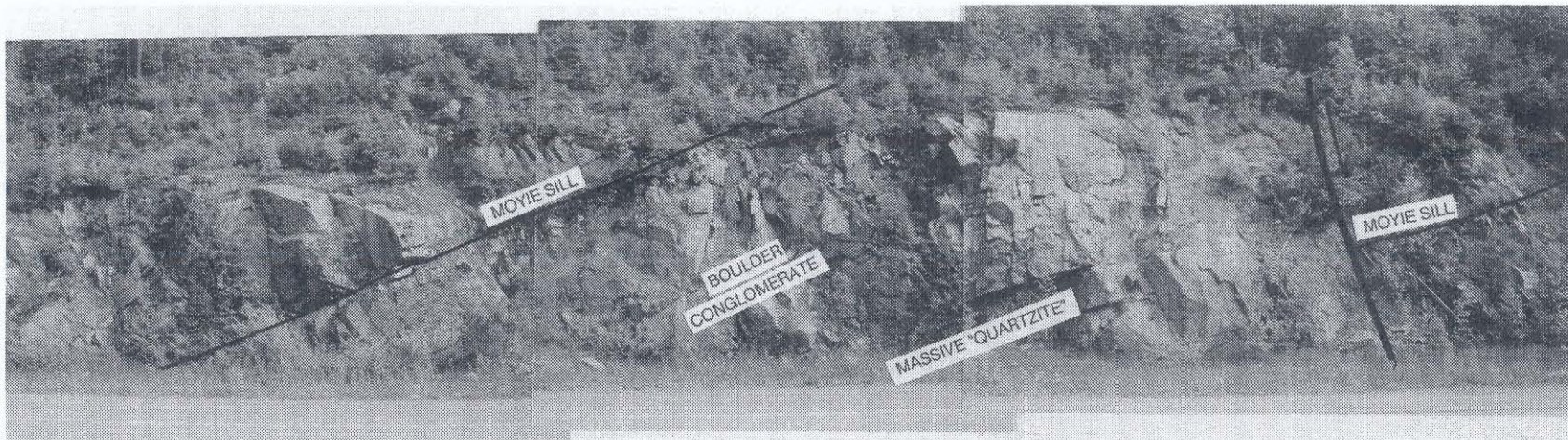


Figure 13. Photograph of roadcut (Stop 1-7) showing relationships of sills to altered and fragmented middle Aldridge Formation.

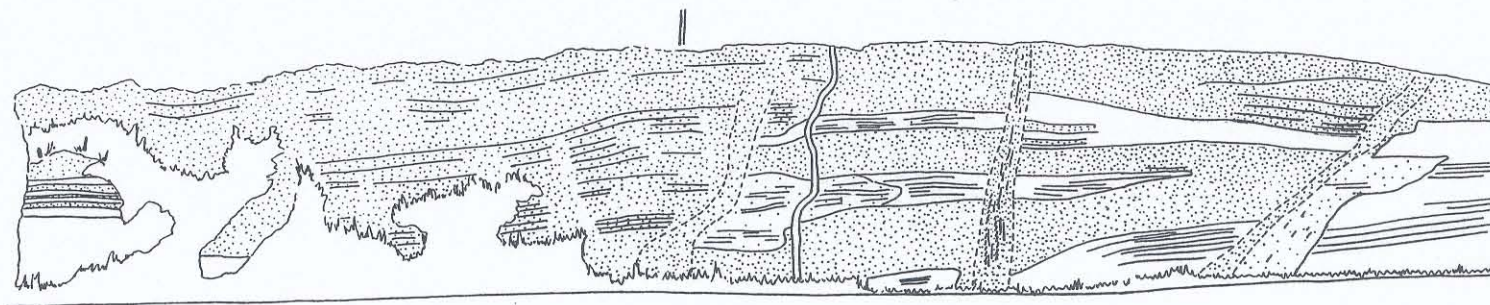


Figure 14. Line sketch of albitite zone, middle Aldridge Formation in roadcut at Stop 1-8. View looks west at southern part of roadcut. Dense stippled areas are massive albitite, open stipple denotes patchy albitite with chlorite-muscovite alteration. The boundaries of discordant zones of massive albitite with abundant fractures are shown in dashed lines. Also shown is a planar lamprophyre dyke that appears curviplanar due to irregular surface of roadcut.

of middle Aldridge strata) relative to the albite suggesting that sulphide predates the albitite alteration and that sulphide does not appear to have been introduced during alteration.

The albitite is interpreted as a fault controlled alteration zone. The closest gabbro sill within underlying strata is exposed several kilometres to the northeast in the Iron Range. However, a gabbro sill occurs upslope, approximately 125 metres stratigraphically above the albitite. This roadcut lies within an anomalous belt of lower and middle Aldridge strata exposed in the Iron Range to the northeast and the Creston Ramparts to the southwest. Within the belt there is an unusual volume of gabbro sills, gabbro dikes, altered rock typically of albite-chlorite composition and fragmental rocks. Some large albitite bodies occur along the margins of gabbro sills.

### Comment:

The origin of albite-chlorite-pyrite alteration is enigmatic. The large volume of albite-chlorite-pyrite alteration within and overlying the vent complex of the Sullivan deposit (Stop 2-1) has been interpreted by some workers to suggest that the albite alteration is related to late stage ore fluids (*e.g.* Hamilton *et al.*, 1983). Turner and Leitch (1992) recognize zoned envelopes of albite-chlorite-pyrite alteration around some gabbro dikes (*e.g.* Red dike) underlying the Sullivan deposit and albitic alteration of some dikes and sills suggesting that alteration post-dated the local intrusion of gabbro. Turner and Leitch *op cit.*) suggest that alteration accompanied intrusion of the gabbro sill complex and that fluids were guided at least in part along sill and dike contacts, as well as along faults resulting in albitic alteration both along gabbro contacts as well as away from them (Figure 20).

Retrace route to Kimberley.

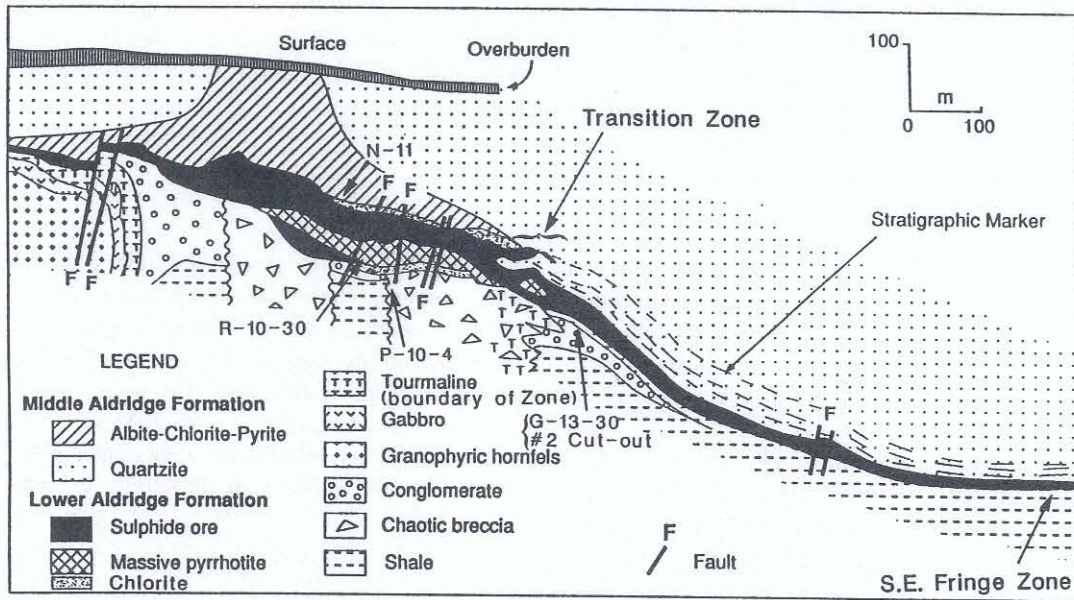


Figure 15. Geologic cross-section of the Sullivan deposit (modified from Hamilton et al., 1982).

## DAY 2: KIMBERLEY AND ST. MARYS VALLEY: PROTEROZOIC HYDRO- THERMAL MINERALIZATION AND AL- TERATION

Day 2 will focus on ore formation and sediment alteration associated with hydrothermal processes by reviewing the geology of the Sullivan mine and the corridor of alteration and fragmentals that extends 6 to 7 kilometres south of the Sullivan mine. We will conclude with a view stop of the gabbro sill complex within strata underlying the Sullivan deposit. Because the number of people that can be accommodated on an underground tour of the Sullivan mine (Trip 2A) is limited, we will run a concurrent trip to the St. Joe prospect (Trip 2B) that exposes discordant fragmental, patchy tourmalinite, and a volcanic tuff that may be an extrusive equivalent of the Moyie sills.

### Trip 2a (morning)

**0.0 km** From the traffic lights at intersection of Ross St. and Wallinger St., Kimberley, drive north on Wallinger St., turning left then immediately right at first stop sign. Follow street past switchback up hill. Continue past hospital and turn left at sign to Sullivan mine. Continue through gates at entrance to Sullivan mine property up hill to Sullivan mine. Park in parking lot on left; the mine office is the first building past the parking lot. MINE TOURS OF THE SULLIVAN MINE MUST BE ARRANGED IN ADVANCE WITH THE MINE STAFF.

### STOP 2-1

#### *SULLIVAN MINE (Sullivan mine staff)*

The Sullivan deposit is one of the largest massive sulphide base metal deposits in the world. It has been described well in a number of papers, recent ones including Ethier *et al.* (1976) and Hamilton *et al.* (1982, 1983) and in guidebooks (Hamilton *et al.*, 1981; Ransom *et al.*, 1985). Therefore, the general description of the deposit is only briefly treated here, and the focus is instead on recent studies on the vent complex (Leitch, 1991, 1992a, 1992b; Leitch *et al.*, 1991; Leitch and Turner, 1991, 1992; Turner and Leitch, 1992). The following summary of Sullivan geology is taken directly from Höy, in press).

The deposit has produced in excess of 134 million tonnes of ore from an original deposit of more than 160 million tonnes that contained 6.5 % lead, 5.6 % zinc, 25.9 % iron and 67 grams per tonne silver (to Oct, 1991). The western part of the orebody is approximately 1000 metres in diameter and up to 100 metres thick (Figure 15). It comprises massive pyrrhotite with occasional wispy layers of galena, overlain by layered galena, pyrrhotite and sphalerite, which in turn is overlain by pyrrhotite, sphalerite, galena and minor pyrite that is intercalated with clastic layers. Its eastern part, separated from the more massive western part by an irregular transition zone, includes five distinct conformable layers of generally well-laminated sulphides separated by clastic rocks. The sulphide layers thin to the east away from the transition zone. Sub-ore grade sulphide layers of pyrite and pyrrhotite with subordinate sphalerite and galena persist beyond the eastern limits of the ore-grade sulphides.

An extensive brecciated and altered zone underlies the massive western part of the orebody (Figure 15). Linear north-trending breccia zones, disseminated and vein sulphides, and extensive alteration to a dark, dense chert-like tourmaline-rich rock are conspicuous

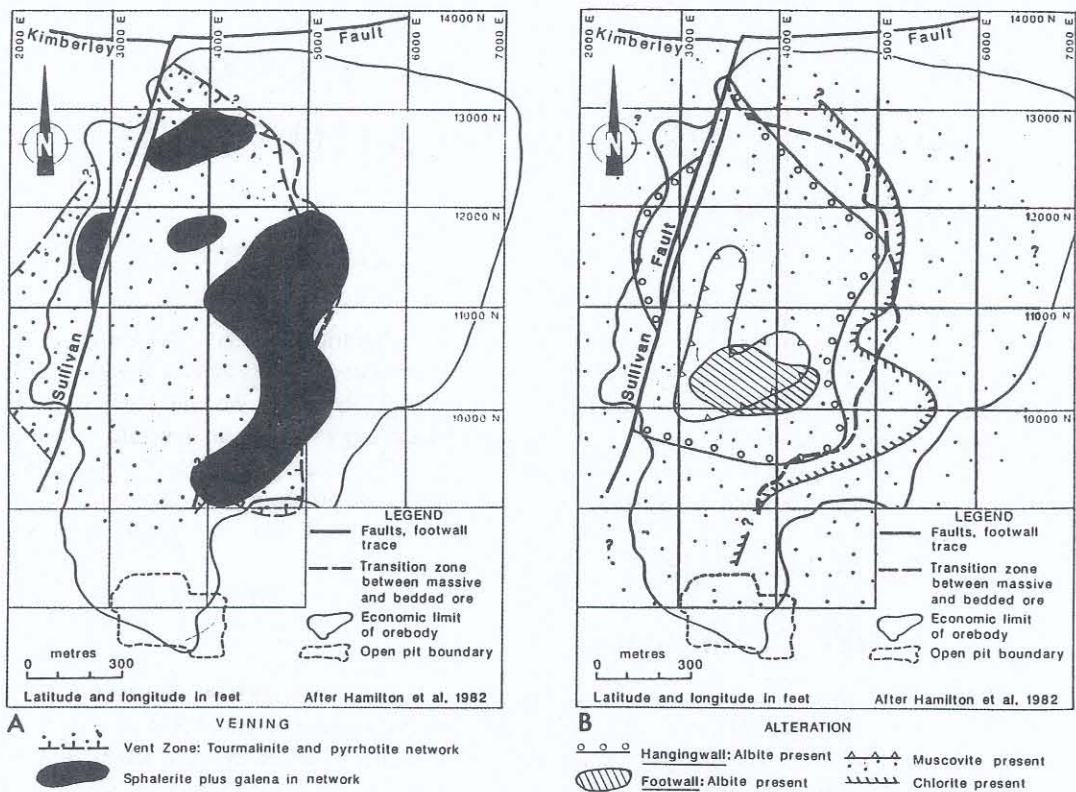


Figure 16. Plan views of the Sullivan deposit showing A) distribution of pyrrhotite-rich and sphalerite-galena-rich footwall mineralization, and B) distribution of albitic and muscovitic alteration in the hangingwall, albitic and chloritic in the footwall (from Leitch and Turner, 1982).

features of the altered footwall. Albitic-chlorite-pyrite alteration is also restricted to the western part of the orebody, occurring in crosscutting zones in the footwall tourmalinite, in the orebody itself and up to 100 metres into the hanging wall (Hamilton *et al.*, 1982; Shaw and Hodgson, *op cit.*).

The deposit is zoned, with lead + silver values decreasing toward the margin in the eastern part. Tin is concentrated in the western part. In general, metal distribution patterns are directly related to proximal chaotic breccia; higher absolute values of lead and silver and higher Pb/Zn and Ag/Pb ratios overlie the breccia zones (Freeze, 1966; Hamilton *et al.*, 1982; Ransom *et al.*, 1985).

Sullivan is interpreted to be a hydrothermal synsedimentary deposit (SEDEX deposit) that formed in a small submarine basin. The western part lies directly above the conduit zone, the brecciated and altered footwall of the deposit.

### Comment (Leitch and Turner)

Stratiform sediment-hosted (SEDEX) Zn-Pb deposits are characterised by bedded zinc and lead sulphides formed as hydrothermal sediments on the seafloor. Some stratiform deposits include a vent complex representing the zone of hydrothermal fluid upflow and discharge at the seafloor during formation of the sulphide sediments, though relatively few studies of such vent complexes are known (*e.g.* Hamilton *et al.*, 1982; Goodfellow and Rhodes, 1990; Turner, 1990). As a consequence, little is known about the chemistry and temperature of fluids that formed stratiform Zn-Pb deposits. Studies in this regard include the Jason (Gardner and Hutcheon, 1985; Turner, 1990), Tom (Ansdell *et al.*, 1989; Goodfellow and Rhodes, 1990)

and Vulcan (Mako and Shanks, 1984) deposits in Yukon and Northwest Territories, and Silvermines (Samson and Russell, 1983) in Ireland.

The Sullivan deposit is a classic example of a stratiform deposit composed of a vent complex overlain and flanked by bedded sulphides. This deposit offers a unique opportunity to study both the ore-forming fluids of a SEDEX deposit and their interaction with the host rocks and bedded sulphides, because of its well-developed vent complex, relatively undeformed state, moderate metamorphic grade and extensive data from underground development and drilling. The vent complex includes a massive pyrrhotite replacement body, an underlying tourmalinite pipe consisting of breccia, altered and fragmented strata and disseminated or veinlet sulphides, and albite-chlorite altered sediments in the hangingwall. Work to date on the tourmalinite pipe includes description (Hamilton *et al.*, 1982), a study of the character of footwall veins (McAdam, 1978) and unpublished studies of alteration (summarized in Shaw and Hodgson, 1980; 1986). Interpretation of tourmalinite formation temperatures, based on oxygen isotope studies, range from less than 100°C (Nesbitt *et al.*, 1984) to 200-250°C (Beatty *et al.*, 1988). Regional metamorphism is biotite-Mn garnet middle greenschist facies at 400°C (McMechan and Price, 1982) and 2.0 kb (5.8-7.6 km depth of burial; Edmunds, 1977).

### Vent complex

The western massive sulphide portion of the Sullivan deposit is underlain by an extensive, in places intensely developed, pyrrhotite-quartz-Fe carbonate stringer network in tourmalinite (Fig. 16; Leitch and Turner, 1992). This probably represents the major fluid upflow zone that formed the deposit. The network ranges from wispy, irregular veinlets that appear to have been emplaced in unindurated sediments at relatively early stages, to planar veins with increasingly abundant quartz and carbonate that appear to have formed at later stages of the development of the feeder zone. A crescent-shaped zone around the margins of this pipe is characterized by the presence of sphalerite and galena in the veinlets (Fig. 16), with associated tourmaline-destructive muscovite alteration. This may represent the site of late-stage fluid flow after sealing of the main central conduit (Fig. 17). Chlorite-dominant veins and alteration envelopes in the footwall and albite-chlorite-pyrite alteration in the hangingwall may be later, related to hydrothermal flow generated by the emplacement of mafic magma at depth below Moyie sills and dikes that are unusually abundant in the footwall of the deposit.

Quartz, and to a lesser extent sphalerite and carbonate, in the network veins, contain abundant secondary or pseudosecondary fluid inclusions (Leitch, 1992a). Inclusions are not seen in wallrock detrital quartz grains that do not appear significantly recrystallized by the greenschist metamorphism. Fluids trapped in the inclusions are probably samples of the mineralizing fluids, in places diluted and/or reset by metamorphism. Mineralizing fluids are characterized as moderately saline 15-27 wt% (NaCl + CaCl<sub>2</sub> + ?MgCl<sub>2</sub>) brines; homogenization temperatures (Th) range from 200-300°C, but may reflect metamorphism. Similar fluids are found at several other prospects (North Star, Quantrell and Kidstar) in Aldridge rocks but fluids in a quartz pod associated with a Moyie sill are of lower salinity. Dilution of the mineralizing brines to wt% NaCl, with mainly low but variable CO<sub>2</sub> + CH<sub>4</sub> by metamorphic fluids, is suspected in several generations of secondary inclusions with Th 200-350°C. Lower temperature secondary inclusions range from 3 to 20 wt% NaCl, Th 90-150°C.

The extensive, in places up to several meter thick, pyrrhotite veins found in the footwall tourmalinite pipe appear to be main feeders to the Sullivan deposit and show similarities to the Stemwinder vein (Leitch and Turner, 1992). The high ratio of sulphide to gangue in the feeder veins directly underlying the Sullivan deposit and in the massive sulphides suggest a concentrated, strong flow of fluid rich in metals combined with a minimal input of detrital material to the basin where sulphide precipitation and deposition was occurring. An analogous situation is the Red Sea Deeps, where a brine pool develops because fluids exhaled on the bottom in restricted basins do not mix with overlying seawater (Ramboz *et al.*, 1988). Instead, they form one or two density-stratified brine layers that cool by conduction to normal seawater without significant loss of salinity. This is a key point, allowing hot, saline exhaled fluids at up to 300°C and therefore lower density than seawater, to form brine pools; regardless of the

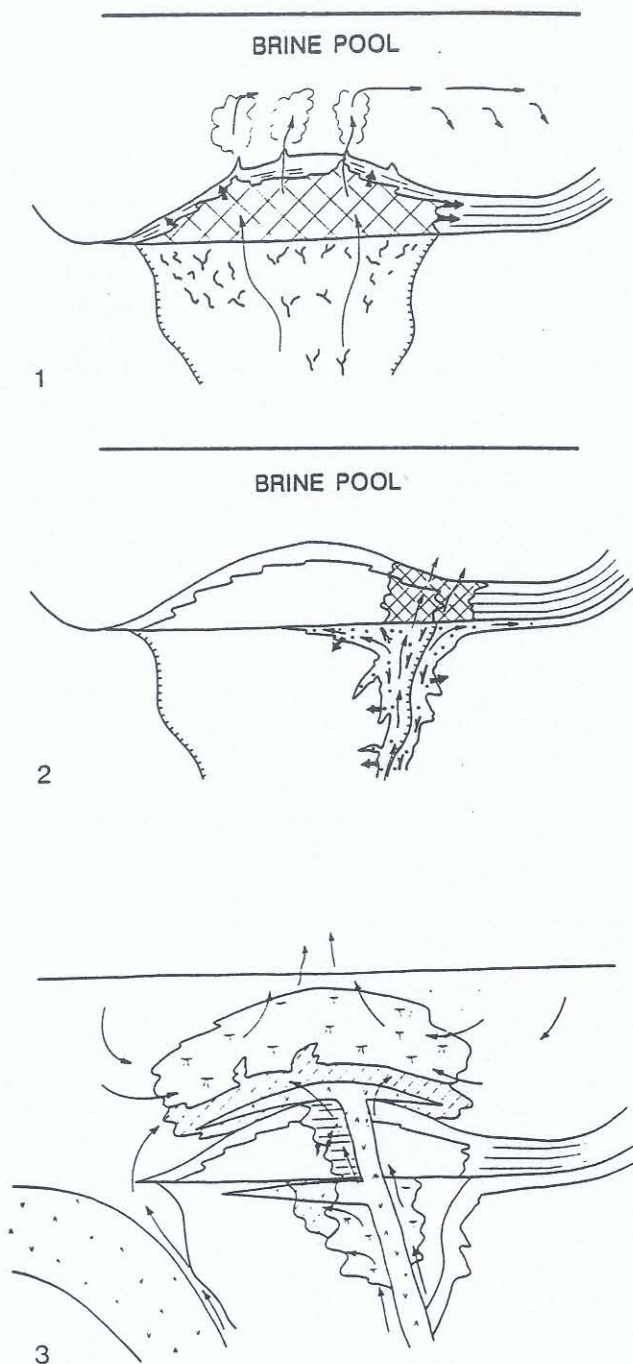


Figure 17. Postulated evolution of the hydrothermal system, Sullivan deposit (from Leitch and Turner, 1992). (1) Main stage hydrothermal flow results in sulphide sedimentation in a brine pool, with progressive replacement of sulphides by massive pyrrhotite and underlying pyrrhotite network/tourmalinite alteration. (2) Late-stage hydrothermal flow is concentrated at the periphery of the main vent zone giving rise to pyrrhotite-sphalerite-galena-sulphosalt veinlets in the transition zone, accompanied by muscovite and ?later chlorite. (3) Post-mineral fluid flow set up by magma body feeding Moyie sills and focused by vertical structures results in albite-chlorite-pyrite alteration.

buoyancy of such fluids, the empirical observation is that mixing does not occur and pools form. Surface waters are at 30°C and bottom water is at 22°C in such a restricted sea, compared to open ocean bottom temperatures of 4°C. Temperatures of Red Sea exiting fluids are not known, but inclusions in anhydrite veins beneath the central portion of the deeps show that boiling occurred, at up to 420°C (Ramboz *et al.*, 1988). It is possible that the first discharge of the hydrothermal system would be cooler than main stage discharge due to conductive cooling, giving rise to a higher density fluid and initiation of the brine pool, which could then not be perturbed by later, hotter, more buoyant fluids (McDougall, 1984).

Such a model for the Sullivan deposit is supported by two key observations. The extremely finely laminated nature of the major portion of the bedded ores, in which details of stratigraphy can be followed for up to 2 kilometres (Hamilton *et al.*, 1982) is suggestive of dewatered Red Sea muds (although plume fallout could also account for the laterally continuous nature of the laminae). If brines trapped in Type 1 and 2 inclusions (Leitch, 1992a) represent the mineralizing fluids, the 15-27 wt% salinities are like those in anhydrite veins underlying the Red Sea brine pools, and similar to the salinity of the brine pools (13.5-25.6%: Ramboz *et al.*, 1988). Although evaporites are not known in the Belt-Purcell Basin, they may have been present at the base of the section, and dissolved during metamorphism (as postulated in the Broken Hill district of Australia: J. Slack *et al.*, unpub. manuscript). Dilute fluids containing a variable carbonic component are likely a metamorphic overprint on the mineralizing fluids.

### Trace metal distribution

At the Sullivan deposit, shown in cross-section in Figure 15, the bedded sulphides are separated from the massive sulphides by the arcuate transition zone which overlies the eastern margin of the footwall tourmalinite-pyrrhotite vent zone. Several minor minerals (cassiterite, stannite, freibergite, arsenopyrite, bismuthian boulangerite and jamesonite, gudmundite, ?bismuthinite, Bi-Sb alloy) rich in Sn, Ag and the semi-metals As, Sb and Bi appear concentrated near the transition zone in veins and disseminations with associated muscovite alteration (Leitch, 1992b). The distribution of Sb which is peripheral to that of As and Sn (Freeze, 1966; Fig. 18) may be explained by the abundance of boulangerite and lesser

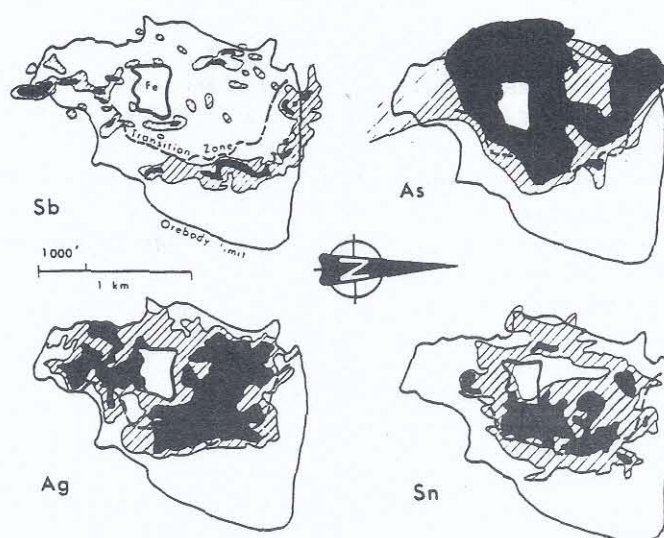


Figure 18. Plan view of Sullivan orebody showing distribution of minor metals (after Ransom, 1977 and Freeze, 1966).

jamesonite in and near the transition zone. Tetrahedrite probably broadens the Sb distribution since it is more common and widespread than boulangerite and jamesonite. Tetrahedrite also controls the distribution of Ag in the orebody; Ag is concentrated over the footwall vent zone inside the transition zone. Preliminary microprobe analyses suggest the principle locus of silver is in freibergite rather than in solid solution in galena as suggested by Freeze (1966) and Hamilton *et al.* (1982).

The distribution of Bi probably lies roughly inside that of Sb, since it is found in bismuthian boulangerite and jamesonite, and native Bi-Sb alloy, within the area delimited by the transition zone. It thus mimics the distribution of arsenic (Fig. 18); the occurrence of the Bi-Sb alloy with arsenopyrite supports this hypothesis. Tin, dependent primarily on the distribution of cassiterite, is concentrated in an annular zone inside the transition zone coincident with higher arsenic concentrations (Freeze, 1966; Fig. 18). Most tin is associated with the pyrrhotite-rich zone at the base of the orebody, with values falling off towards the hangingwall (Freeze, 1966). In this study both cassiterite and stannite were observed near the base of the deposit in footwall rocks or massive pyrrhotite, within an area bounded by the transition zone. The association of tin-bearing minerals with muscovite or arsenopyrite-bearing cross-cutting structures suggests that Sn, along with As, Bi, and possibly Sb, is related to late-stage upflow of hydrothermal fluids in the transition zone (Leitch and Turner, 1992). The association of Ag with this process is less clear, although Ag appears to be primarily controlled by the distribution of tetrahedrite that also contains significant amounts of Sb.

Cd, In, Tl and a portion of the Mn in the Sullivan deposit are probably contained within and controlled by distribution of sphalerite. Up to 0.3 wt% Cd was detected in sphalerite; further work is required to determine if the 0.05-0.08 % In level is real. Coincidence of maximum concentrations of Tl with Zn-rich areas suggests Tl occurs in sphalerite. Ga and Ge recovered in minor quantities at the Trail smelter probably are also hosted in sphalerite, although this was not tested in this study. These elements are probably at levels too low to be detected except by the most rigorous microprobe analysis employing high beam currents and long counting times.

## Zonation

Preliminary analyses from limited numbers of samples suggest zoning of mineral compositions that give several vectors of potential use to exploration: sphalerite to higher Fe inside the transition zone, and both carbonate and garnet to higher Mn towards the fringes of the Sullivan deposit. Manganese enrichment occurs peripheral to other stratiform sediment-hosted Zn-Pb deposits, such as Meggen in Germany (Gwosdz and Krebs, 1977) or Tynagh in Ireland (Russell, 1974), and is known to concentrate distally in the Red Sea muds (Zierenberg and Shanks, 1988). This suggests elevated Mn content peripheral to the Sullivan and North Star deposits is due to Mn-rich exhalations. Metamorphic recrystallization has concentrated the Mn into certain preferred phases such as garnet and carbonate, and to a lesser extent tremolite, diopside, chlorite, biotite and epidote. Garnet formed preferentially during metamorphism in the Sullivan-North Star altered corridor because of elevated Mn content of the altered strata (Leitch *et al.*, 1991). Thus the simple picture of a manganese "halo" surrounding the Sullivan deposit has been modified and blurred, mainly by widespread exhalation from several centers surrounding the deposit, and by local metamorphic redistribution. Whole-rock analyses for Mn around the Sullivan deposit and in the Aldridge show complex trends possibly due to mobilization of Mn into variable minor carbonates (J. Hamilton, pers. comm., 1991).

Trends are also apparent in Fe content of minerals such as chlorite, epidote and possibly biotite in the Sullivan-North Star deposits and surrounding altered rocks. The Fe content of epidote increases slightly from regional unaltered rocks to the altered corridor. Also, Fe contents in chlorites are highest in massive sulphide samples, associated with minor occurrences of Fe-rich chlorite (chamosite) and biotite (lepidomelane). This is in contrast to the observed decrease in the Fe content of most silicates towards the center of other metamorphosed massive sulphide deposits, predicted due to greater affinity of sulphides for Fe in the competition between sulphides and silicates (Nesbitt, 1986).

The occurrence of anorthite in tourmalinized rocks near North Star compared to regional andesine or oligoclase is difficult to explain. The process of tourmalinization may remove Na<sub>2</sub>O, resulting in feldspar enriched in CaO. Widespread albite in altered rocks in the hangingwall and less commonly the footwall at Sullivan appears to be related to hot fluids mobilized by intrusion of Moyie sills and dikes and focused along vertical structures, after emplacement of the orebody (Turner and Leitch, 1992).

Tourmaline as both regionally distributed, coarse, possibly detrital grains and fine hydrothermal needles is intermediate in composition between schorl and dravite. Coarse, pale yellow-brown tourmaline probably closer to dravite in composition (10% MgO; Ethier and Campbell, 1977) is found in (1) matrix to breccia clasts at the base of the massive pyrrhotite body and (2) where albitization has recrystallized tourmalinite in both footwall and hangingwall. These relations suggest that recrystallization of early formed tourmaline is by ongoing hydrothermal alteration and heat flow generated by Moyie sills (Turner and Leitch, 1992) rather than "related to uneven heat flow during metamorphism" (Ethier and Campbell, 1977, p. 2348). Tourmalines related to massive sulphides are distinctly Mg-rich, approaching end-member dravite, and are not thought to be greatly altered by subsequent metamorphism due to the refractory nature of tourmaline (Taylor and Slack, 1984). The compositions of regional and hydrothermal tourmaline are also similar, respectively, to sulphide-free tourmaline of the Broken Hill Group tourmalinites and sulphide-rich tourmalines of the Globe mine tourmalinite at the northern end of the Broken Hill lode, Australia (J. Slack *et al.*, unpub. manuscript).

### Albite-chlorite-pyrite alteration and relationship to gabbro intrusions

Chlorite-albite-pyrite alteration cuts the tourmalinite pipe, Sullivan orebody and overlying strata (Figures 15 and 19; Turner and Leitch, 1992). The root zone of this alteration coincides with set of dikes and sills, apophyses of the larger footwall gabbro sill (Figure 20). Alteration postdates intrusion as some dikes and sills are locally altered. Altered sedimentary rocks adjacent to gabbro are zoned from proximal albite-chlorite to chlorite-pyrite. The ascent of Na-rich, Mg-depleted hydrothermal fluids followed dikes in the Sullivan orebody localizing albitic alteration (Figure 20). Fluids may be related to deep gabbro intrusions below the Moyie sill complex. Mixing with Mg-rich seawater caused peripheral chloritic alteration, and late collapse of the hydrothermal system caused chloritic alteration to overprint earlier-formed albitic alteration (Figure 20). Southwest of the Sullivan mine, albite-chlorite alteration extends 200 m above the contact of a gabbro sill. The absence of base metals suggests albite-chlorite-pyrite alteration is not directly related to ore-forming processes.

Höy (1989) suggested that the Moyie sills were intruded into unconsolidated Aldridge sediment and proposed the Guaymas sedimented rift basin as a modern analogy. Basalt sill complexes are known to intrude modern sediments to within tens of metres of the present seafloor (Einsele, 1982; Gieskes *et al.*, 1982; Zierenberg *et al.*, in press). A model for intrusion by Einsele (1982) assumes upward-younging sills as each subsequent magma injection rises to the top of previously altered sediment, achieves neutral buoyancy and spreads laterally. Such sills are only slightly younger than the sediments they intrude. One might speculate therefore, that the minimum age of the two gabbro sill complexes exposed southwest of the Sullivan mine (Leech, 1957) can be dated by the stratigraphic level of the uppermost sill of each complex; an older intrusive event up to the time of formation of the Sullivan deposit, and a younger event during middle middle Aldridge time. Such a scenario raises the larger question of the role of the source magma for the Moyie sills as a heat engine of fluids that formed the Sullivan orebody, as suggested by Hamilton (1984). Here we restrict ourselves to the possible relationship of intrusions to albite-chlorite-pyrite alteration.

The upward termination or "silling out" of small gabbro dikes within or immediately above the Sullivan orebody, and the intrusion of the footwall sill up to the base of the orebody suggests that local gabbro intrusion took place when the Sullivan sulphide body was only buried a short distance below the seafloor, as suggested by Hamilton *et al.*, (1982). During early burial, the indurated footwall sediments and thick sulphide mass of the Sullivan deposit would have had a significantly higher density than overlying turbidite sediments. Magma rising

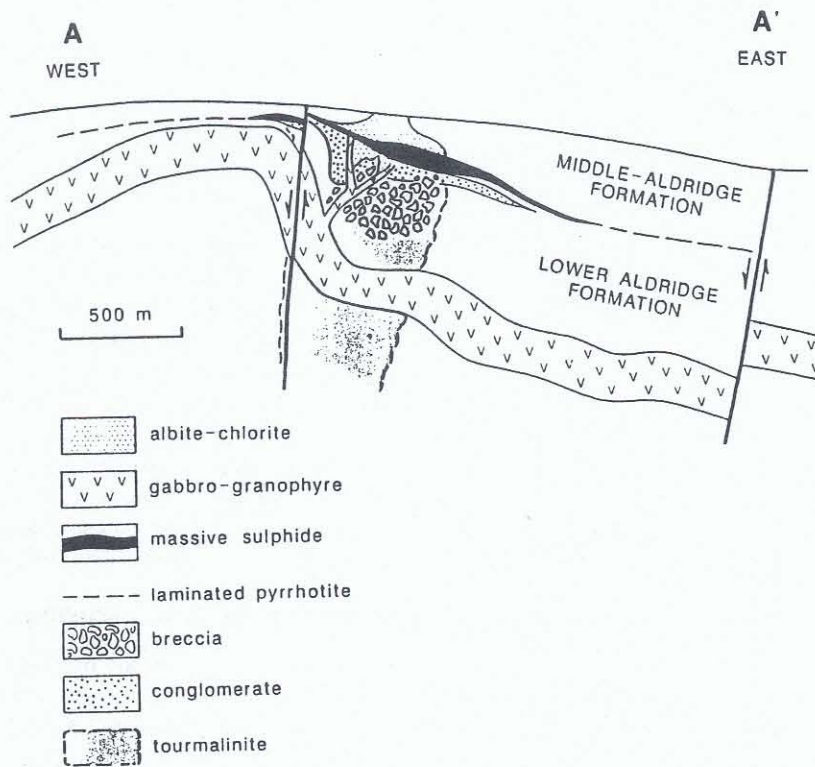


Figure 19. Schematic east-west geological cross-section illustrating the relationship of the gabbro arch to the Sullivan ore-body (modified from Hamilton, 1984).

through the indurated tourmalinized footwall sediments and massive sulphide body achieved neutral bouyancy at the base of overlying partly lithified silts and muds and did not rise further.

Many of the small dikes and sills within the Sullivan mine are altered in part to an albite-chlorite or chlorite-pyrite assemblage and this alteration clearly post-dates these intrusions. Zoned envelopes of albite-chlorite-pyrite alteration in sedimentary rocks adjacent to dike and sill contacts suggest either alteration occurred during gabbro intrusion, or that later flow of hydrothermal fluids was localized along intrusion contacts. It is considered unlikely that alteration occurred during intrusion given the small size of the dikes, the significant addition and removal of components during alteration, the absence of such albite-chlorite alteration associated with most Moyie intrusive contacts throughout the Aldridge Formation, and the minimal alteration associated with modern sills intruded into wet sediments (*see below*). Albite-chlorite alteration is superimposed on tourmalinite, the massive sulphide body and siliciclastic strata up to the present erosional surface 150 metres above the Sullivan orebody. Alteration must be at least as young as these youngest altered rocks. Using modern rates of deposition of 100 to 2000 cm/1000 years for active turbidite depocentres (*e.g. Luternauer et al., 1983*), the 150 metres of thick-bedded turbidites overlying the Sullivan deposit might represent between 7500 and 150 000 of years of deposition. This suggests that the youngest albite-chlorite alteration is at least 10 000-150 000 years younger than ore formation.

Footwall albite-chlorite altered rock, the root of the alteration zone that transgresses the Sullivan sulphide deposit and hangingwall, is centered on the cluster of gabbro dikes and sills. The position of the dike set appears to have localized the plume of rising hydrothermal fluids. Zoned alteration envelopes noted on individual dikes indicate fluid flow was channeled along intrusion margins. We presume that these dikes would connect with the steeply dipping

discordant limb of the footwall sill at depth and that hydrothermal fluids ascended along this discordant intrusive contact (Figure 20).

It is worth comparing these relationships with studies in the Guaymas Basin, a modern sedimented submarine rift zone intruded to shallow levels by sills and plugs where two types of hydrothermal system are recognized (Gieskes *et al.*, 1982). Shallow sills emplaced in the Guaymas Basin sediments produce relatively low-temperature (<200°C), short-duration hydrothermal cells created by expulsion of ambient pore water (Einsele, 1982) and minor alteration of adjacent sediments (Gieskes *et al.*, 1982). However, sediments altered to a greenschist-facies metamorphic assemblage were intersected below 190 metres depth in a hole drilled to 250 metres (Kelts, 1982; Gieskes *et al.*, 1982). With increasing depth, turbidite sediment is progressively altered to anhydrite-dolomite, illite-chlorite-pyrite, chlorite-pyrite-calcite, and chlorite-epidote-quartz-albite-pyrrhotite-sphene (Kelts, 1982). This alteration is interpreted to reflect the upflow zone of a second much larger hydrothermal circulation system (300°C) driven by large magmatic intrusions at depth and recharged by deeply circulating seawater (Gieskes *et al.*, 1982). Sills can act as a lid on such deeper fluid flow, and lead to lateral channelling of fluids to zones of cross-stratal permeability such as faults, fractures and sill margins (Einsele, 1982; Geiskes *et al.*, 1982). Discordant intrusive margins disrupt the

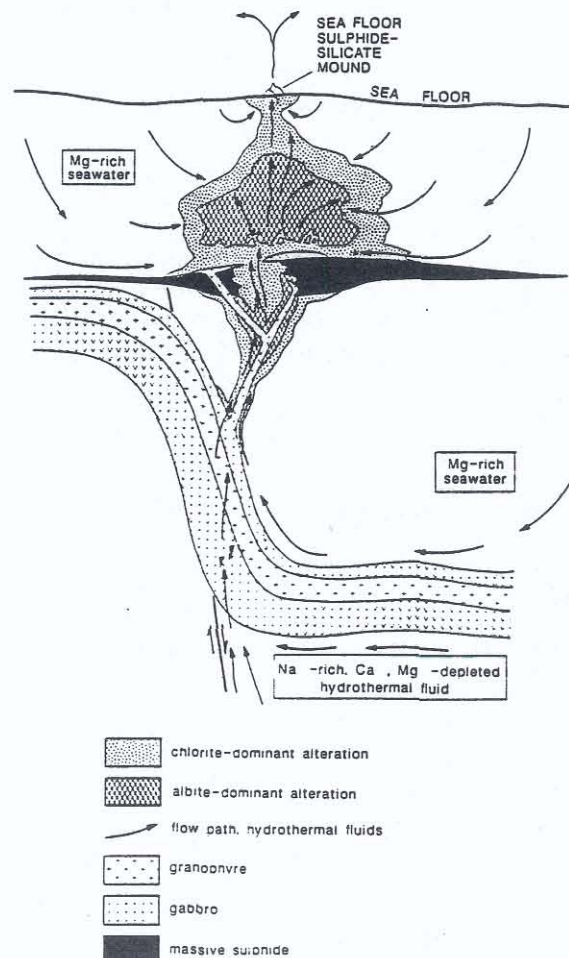


Figure 20. Schematic interpretation of geological environment during formation of albite-chlorite-pyrite alteration (Turner and Leitch, 1992).

natural lateral permeability of sediments, and are zones of cross-stratal permeability (Einsele, 1982), as indicated by the abundance of submarine hydrothermal deposits along the margins of seafloor hills underlain by shallow level sills (e.g. Zierenberg *et al.*, in press).

During emplacement of the Moyie syn-rift intrusive complex, hydrothermal circulation driven by intrusions below those presently exposed (sedimentary rocks adjacent to most sills in the Aldridge Formation are not significantly altered) is interpreted to have moved laterally at the base of overlying sill sheets, and ascended along fault zones such as the west side of the Sullivan sub-basin. At Sullivan, these fluids appear to have followed the steep contacts of the footwall sill and branching dike apophyses, resulting in the hydrothermal plume focusing upwards on the orebody and overlying strata. Maximum alteration occurs at sill contacts and diminishes away from them, suggesting fluid flow along and upward from the contact. Steeply dipping albite veinlets in the altered rocks indicate that subvertical fluid flow was important, possibly related to an unrecognized fault that breached the sills and allowed heated fluids from below the sills to rise into overlying sediments.

Albite-chlorite alteration is distinguished by elevated Na<sub>2</sub>O (7%); chlorite-pyrite by elevated MgO (13%) and total Fe (29%). Both alteration types are significantly depleted in SiO<sub>2</sub>, K<sub>2</sub>O and CaO relative to unaltered Aldridge strata (Hamilton *et al.*, 1982). Formation of Mg-silicates in seafloor hydrothermal systems relate to high temperature mixing of Mg-bearing seawater and Mg-depleted silica-rich hydrothermal fluids (Seyfried *et al.*, 1988). Mg uptake by secondary phases makes it unlikely that seawater-derived Mg will penetrate significantly into the high temperature regions of submarine geothermal systems. The chloritic alteration at Sullivan therefore likely was produced by a seawater dominant system. Experiments by Bischoff *et al.* (1981) monitored the reaction of greywacke with seawater and brines at 350°C and 500 bars and indicate that an assemblage of chlorite-smectite-albite can form from heated seawater. However, the formation of extensive bodies of massive albite (*i.e.* albitite) with little chlorite likely requires brines enriched in sodium (Bischoff *et al.*, 1981) and significantly depleted in Mg and Ca, unlike seawater (Seyfried *et al.*, 1988). Sodium fixing through albitization is expected in upflow zones of seafloor hydrothermal systems in which Si-rich, Mg-free and Ca-depleted fluids form during high-temperature reactions at depth to form epidote-quartz-chlorite assemblages (Seyfried *et al.*, 1988). Early formed proximal albite occurs along hydrothermal conduits surrounded by chlorite-rich assemblages, and is locally overprinted by late chlorite veins. This suggests albitic alteration reflects the core of the upflow zone of high Na/(Mg + Ca) brines (Figure 20). On the margins of this hydrothermal plume, mixing with entrained Mg-rich seawater-derived interstitial fluids resulted in chlorite-dominant alteration. During the late stages, collapse of the hydrothermal plume allowed penetration of Mg-rich seawaters into the altered rock body along fractures, particularly at the base of the massive albite causing chloritic alteration to overprint albite.

## Trip 2b (morning)

- 0.0 km Intersection of Ross St. and Wallinger St., Kimberley. Drive south on Wallinger (Highway 95A).
- 5.8 km Intersection, St. Marys Lake Road. Continue on 95A.
- 6.7 km Marysville
- 15.3 km Junction, Wycliffe Road
- 21 km Bridge over St. Marys River
- 26.2 km Railway overpass
- 28.3 km Junction of Highways 95A and 95/3. Take onramp onto Highway 95/3 heading south. Drive through Cranbrook following signs for Highway 95/3 (at second lights turn right).
- 37.4 km Travel Information Center (east side) and Jim Smith Road (west side).
- 42.4 km Bluffs to west expose gabbro (Höy and Carter, 1988).

- 40.3 km** Junction, unmarked gravel road (marked Fassifern Road on tree 50 m beyond railway crossing). Turn west onto Fassifern Road, cross railway tracks. Road turns south, then north and enters a large clearcut area. Look for dirt track that joins road obliquely from the southwest.
- 43.3 km** Junction of dirt track from southwest with gravel road. Four-wheel drive advised from here on. Turn west onto dirt track. Track ascends slope, at times across shelf rock.
- 45.2 km** Intersection with north-south track. Continue on track (westwards).
- 45.8 km** Branch track to left (just past outhouse on left). Take left branch and park. Continue walking down branch 100 m to cleared area outcrop (Figure 1).

## STOP 2-2

### 45.9 km: *VOLCANIC TUFF, CHANNEL COMPLEX, ST. JOE PROPERTY (Höy)*

A discordant zone of fragmentals cutting across middle Aldridge turbidites and siltstone is exposed in outcrop in the cleared area (Pighin, 1983). The fragmental unit has been trenched and cross-cutting veins have been explored by a short adit. A detailed surface map (Figure 21) shows that it comprises a number of fining upward cycles, each with a coarse base that scours the underlying unit, and each generally capped by a finer grained laminated or massive unit. The fragmental succession pinches out to the south; its maximum thickness, in the northern part of the trench, is greater than 16 metres.

Measured sections through the fragmental succession (Figure 22) clearly show the graded nature of individual units and truncations by successively younger units. The coarsest unit (Unit F) occurs near the top of the pile above the thickest part of the succession. Subrounded blocks up to 10 centimetres in long dimension occur within a finer-grained granular matrix. Occasional clasts have well-defined rims, comprising dominantly chlorite and minor plagioclase. The clasts have variable compositions and textures; none, however, are similar to the Moyie sills. Some clasts comprise dominantly chlorite whereas others contain feldspar and quartz phenocrysts; others comprise a granular mixture of dominantly feldspar and chlorite. The groundmass is primarily broken feldspar and quartz crystals with abundant biotite and chlorite. This fragmental is interpreted to be a reworked tuff breccia that grades upward into a lapilli tuff. Blocks with rims may be fragments of pillows or, alternatively, armoured lapilli with probable alteration of glass to chlorite. Similarly, chloritic clasts may originally have been glass shards.

Other fragmental units are finer grained but are also typically graded. They scour and locally deform underlying units. They are mineralogically similar to the groundmass of Unit F, with abundant broken feldspar and quartz crystals and numerous small angular, aligned chlorite-rich clasts.

A projected section of the upper fragmental, based on the surface map and measured sections, is shown in Figure 23. It illustrates its cross-cutting nature and suggests deposition as successive surges or, more likely, as channel deposits; the inferred deep-water environment of the middle Aldridge precludes surge deposition. Hence, it is concluded that this fragmental succession comprises dominantly reworked, water-lain lapilli and crystal tuff or tuffaceous conglomerate and sandstone. It is the only known volcanic unit within the Aldridge Formation. However, as it is associated with abundant, probably comagmatic high-level sills, the Moyie intrusions, it may simply record phreatic explosion in a shallower water environment. But the presence of significant quartz, possibly even as phenocrysts, suggest a more felsic magma source than the Moyie sills.

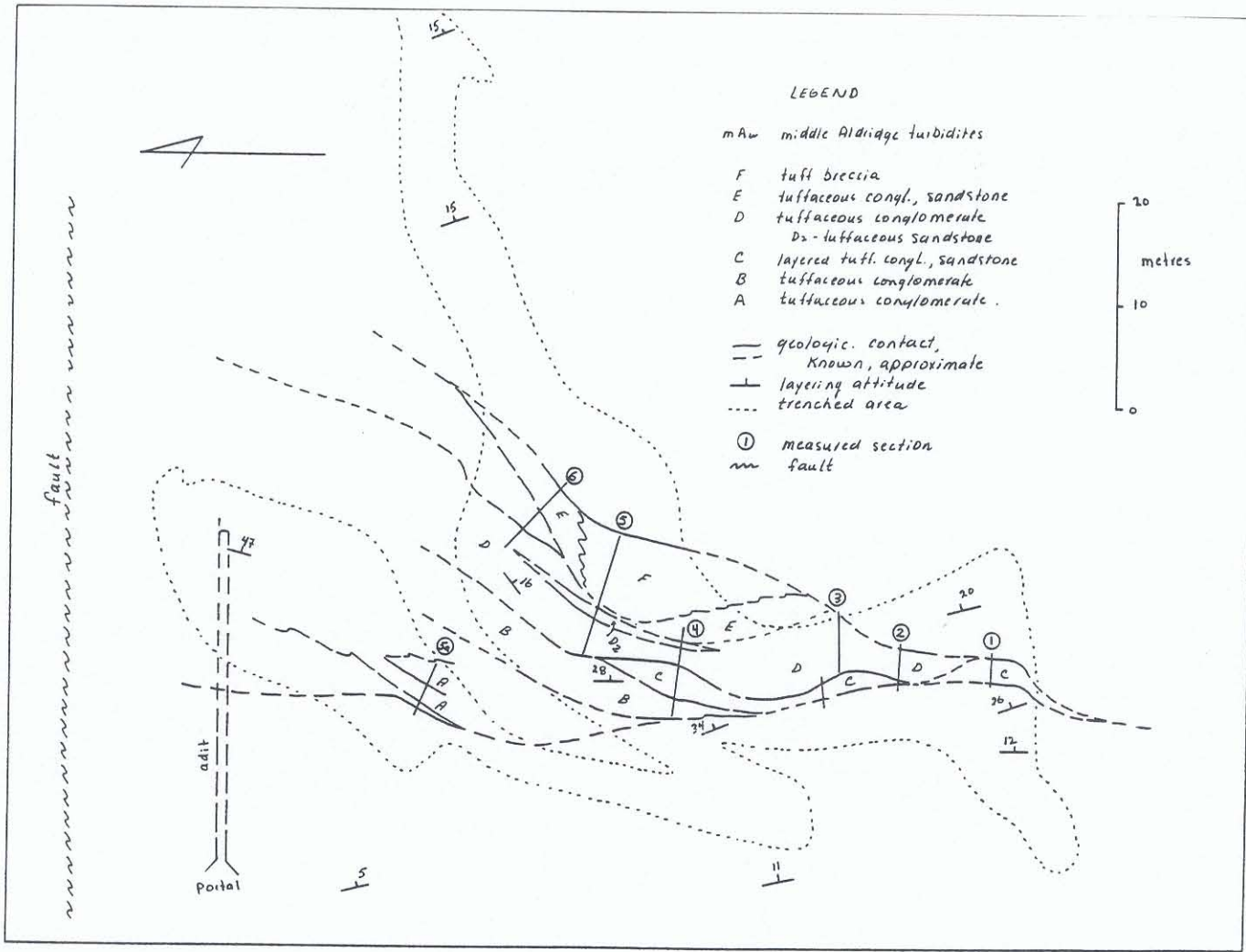


Figure 21. Geological map of the upper fragmental, St. Joe prospect (modified from Pighin, 1983).

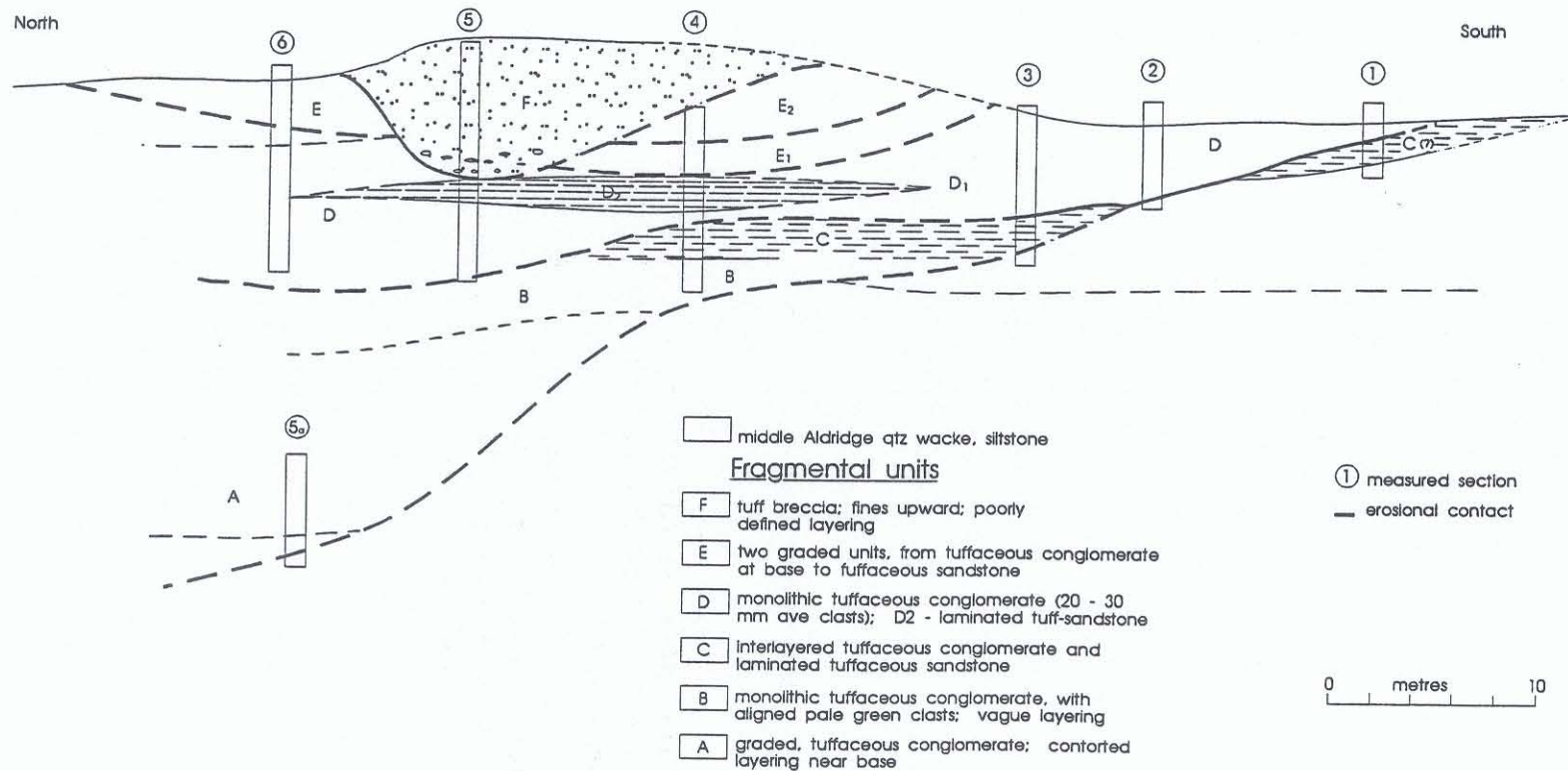


Figure 23. An interpretive section through the upper fragmental, St. Joe prospect.

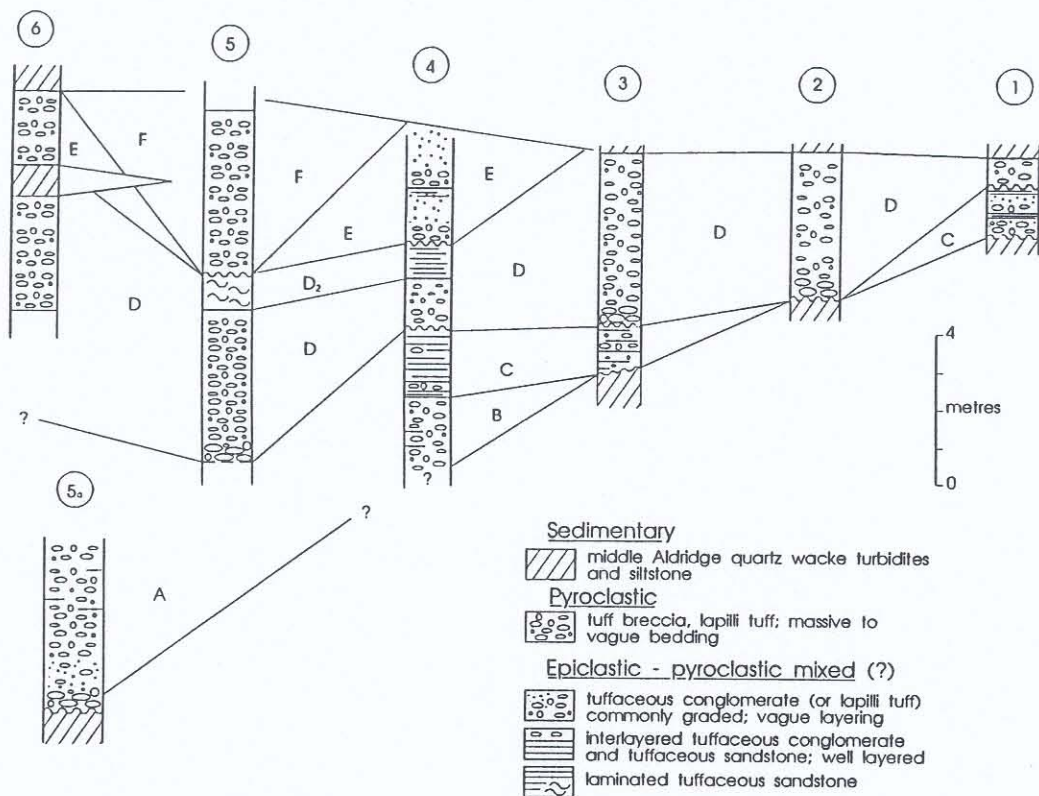


Figure 22. Measured sections through the upper fragmental, St. Joe prospect

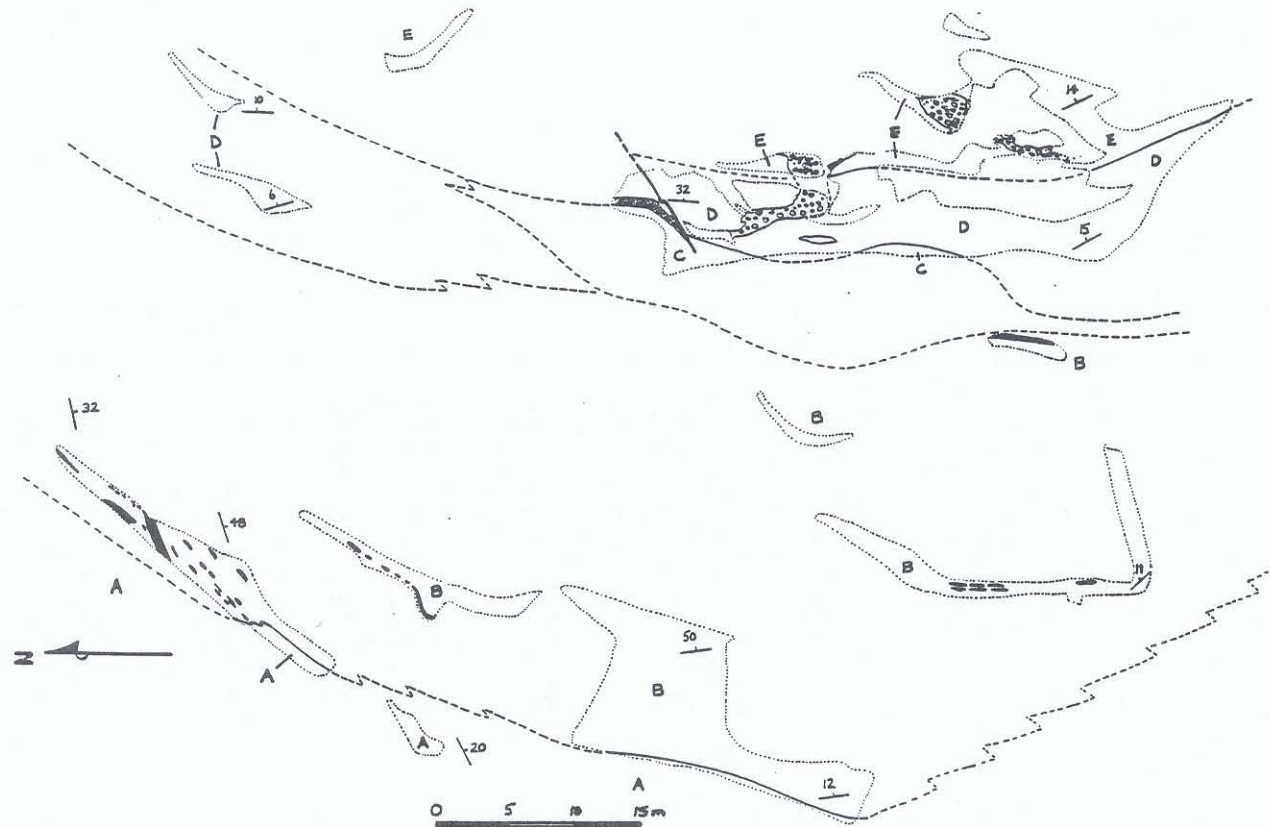
## STOP 2-3

### 46.6 km: **DISCORDANT BRECCIA, CARBONATE-SULPHIDE AND TOURMALINITE ALTERATION, ST. JOE PROPERTY** (R. Turner, C. Leitch)

From parking site at upper fragmental return to main dirt track. Continue west and down hill 0.7 km to junction with track on left (south). Turn onto south track and park. Track is covered with several deadfalls. Follow track across bottom of ravine and up other side. Continue for about 300 m to cleared area with low rock exposures.

At this stop we visit an excellent exposure of a discordant breccia associated with anomalous carbonaceous strata and small tourmalinite bodies within the Middle Aldridge Formation (Pighin, 1983). The fragmental occurs within northwest-striking, shallowly east-dipping strata about 700 metres southwest of, and 300 metres below the stratigraphic level of, the volcanic tuff of the previous stop. The fragmental lies about 150 metres above the stratigraphic level of a gabbro sill exposed 250 metres to the southwest in the valley of Kiakho Creek.

The fragmental bodies occur within a carbonate-bearing dark grey wacke (Unit D, Figure 24) and overlying black argillaceous wacke with abundant disseminated pyrrhotite (Unit E, Fig. 24) that are exposed in low outcrop within the cleared area. These units are underlain by a highly carbonaceous wacke (Unit B, Fig. 24), a highly unusual lithology for the Middle Aldridge Formation, that contains small subconcordant lenses of black and pale tourmalinite. The carbonaceous wacke and tourmalinites are exposed downslope to the west from the cleared area on cliff faces and road cuts.



**LEGEND**

- |   |  |   |  |
|---|--|---|--|
|  | Tourmalinite, black to brown   |  | Thick bedded wacke; pale grey, rusty weathering                      |
|  | Pyrrhotite-rich fragmental rock  |  | Black carbonaceous wacke: thin laminated with white siliceous layers |
|  | Fragmental; angular to rounded clasts to 5 cm of wacke, pale tourmalinite and massive sulphide   |  | Quartzitic wacke: grey, medium-bedded, rusty weathering              |
|  | Black argillaceous wacke; laminated, rusty weathering, abundant disseminated pyrrhotite, some laminated pyrrhotite                                   |   |  |
|  | Medium to thin bedded wacke; dark grey, rusty weathering, parallel laminated, some disseminated pyrrhotite, pitted carbonate-style weathered surface |   |  |

Figure 24. Geological map of the area of lower fragmental and tourmalinite, St. Joe prospect (modified from Pighin, 1982).

The main fragmental body is a steeply dipping, northwest trending body 1 to 2 metres wide with several irregular subconcordant lenses that extend along bedding to the north and south. Just to the north is a massive pyrrhotite lens 4 x 0.3 m that contains lithic fragments and appears to be a sulphide-rich concordant breccia. The fragmental is composed of rounded granule to pebble sized clasts in a matrix of fine-grained wacke with larger angular clasts of wacke to 30 cm. A number of rounded clasts, up to pebble size, of tourmalinite and massive pyrrhotite occur locally. Adjacent to the fragmental body, strata are locally veined, brecciated or plastically deformed.

Retrace route to Kimberley

## **Trip 2 (afternoon)**

### **Start Point**

---

**0.0 km** From the traffic lights at intersection of Ross St. and Wallinger St. in Kimberley drive north on Wallinger St., turning right at first stop sign. Follow street past switchback up hill. Continue past hospital and turn left at sign to Sullivan mine (corner grocery on left at corner). Continue to gates at entrance to Sullivan mine property. Park on gravel pullout on left (south) side just before Cominco mine gate. Walk west a short distance past gate to overlook area.

### **STOP 2-4**

---

#### **VIEW OF NORTH STAR-SULLIVAN ALTERATION-FRAGMENTAL TREND (Turner, Höy, Leitch)**

The view looks west across the slopes of North Star Mountain and the Kimberley Ski Resort (Figure 25). Altered and fragmented rocks of the Sullivan-North Star corridor are exposed on the lower part of the mountain and marked by the extent of brown iron stained soils exposed on the cleared ski runs. Altered rocks are exposed from about the halfway point up the mountain to the base of the slope where they are covered by a bench of Pleistocene tills.

The uppermost slopes of North Star Hill are underlain by unaltered east-dipping lower Aldridge strata cut by a variably developed steep, west-dipping cleavage (Figures 25, 26 and 27). The western (upper) boundary of the alteration corridor is coincident with north-trending mineralized structures (Midnight, Kellogg and Quantrell veins) and the stratiform and discordant orebodies at the North Star mine (Figures 25 and 26). Below this line, fragmental or massive unbedded units are common and rock variably altered and mineralized. The mine dumps of the North Star mine have largely been recontoured but are still visible south of the chairlifts. A large area (400 by 400 m) of patchy tourmalinite and elevated base metal content occurs to the north of the white slide that switchbacks down the lower slope covers the northern part of the lower slopes of the ski area. This tourmalinite zone is onstrike with and may be continuous with tourmalinite that forms an envelope on the north-trending Stemwinder vein. The Stemwinder mine area is just out of view to the north on the south side of Mark Creek (Figure 25).

## **Comment**

The zone of alteration within the lower Aldridge Formation, 6 km long by up to 2 km wide, extends south-southeastward from the Sullivan deposit to the North Star Hill area. The north-dipping Kimberley fault, estimated to have over 2500 m of net normal slip, truncates this alteration zone to the north. The zone is characterized by (1) widespread feldspar-destructive muscovite alteration, (2) increased disseminated pyrrhotite, (3) abundance of fragmental rocks, and (4) scattered pyrrhotite-pyrite-sphalerite-galena veinlets. Within the zone are areas up to 100s of metres in dimension of tourmalinite and albite-chlorite-pyrite alteration. The

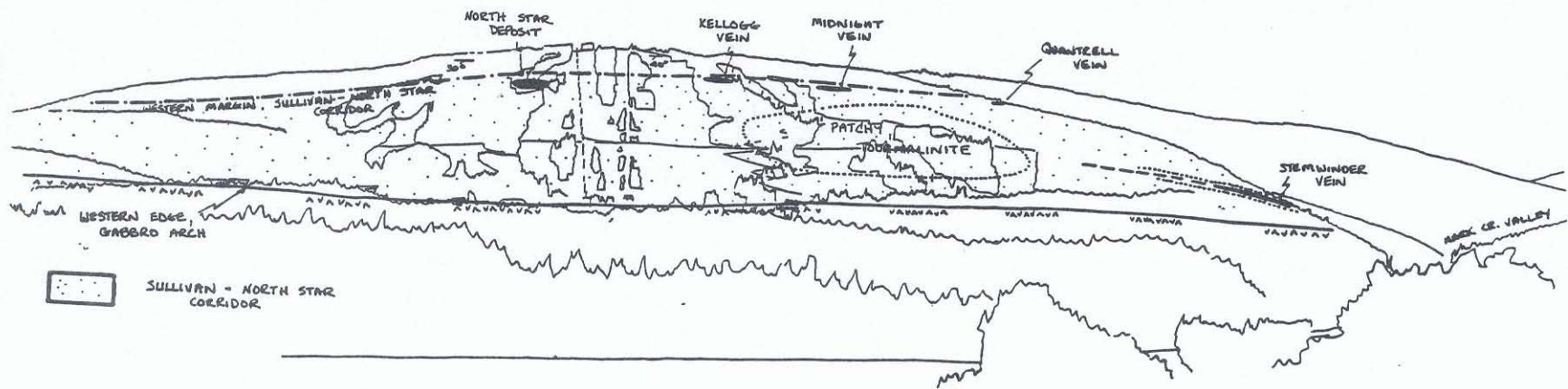


Figure 25. View looking west of North Star Hill and Sullivan - North Star corridor from Sullivan mine road (Stop 2-4).

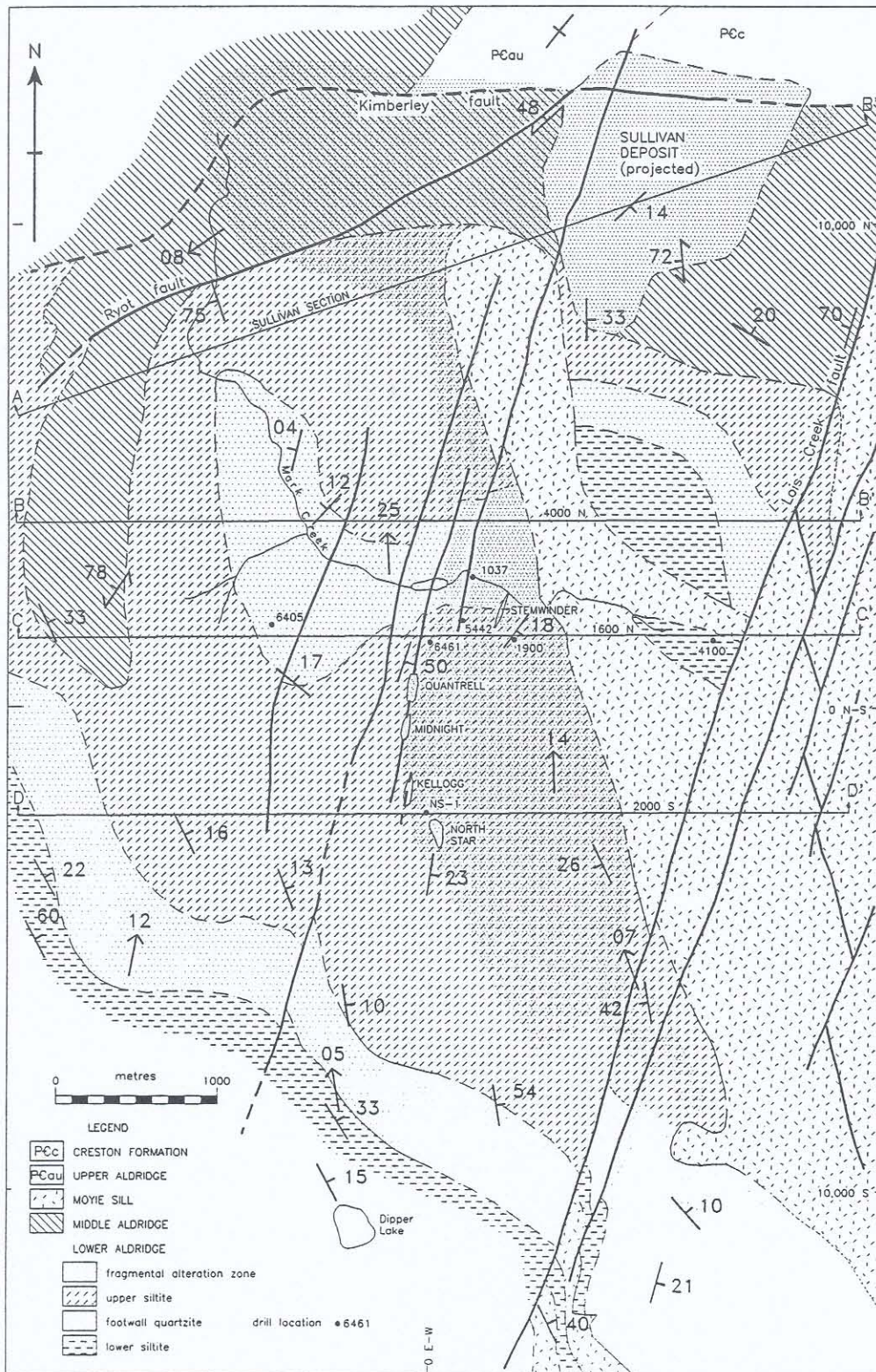


Figure 26. Geologic map of Sullivan - North Star trend (Höy, in press).

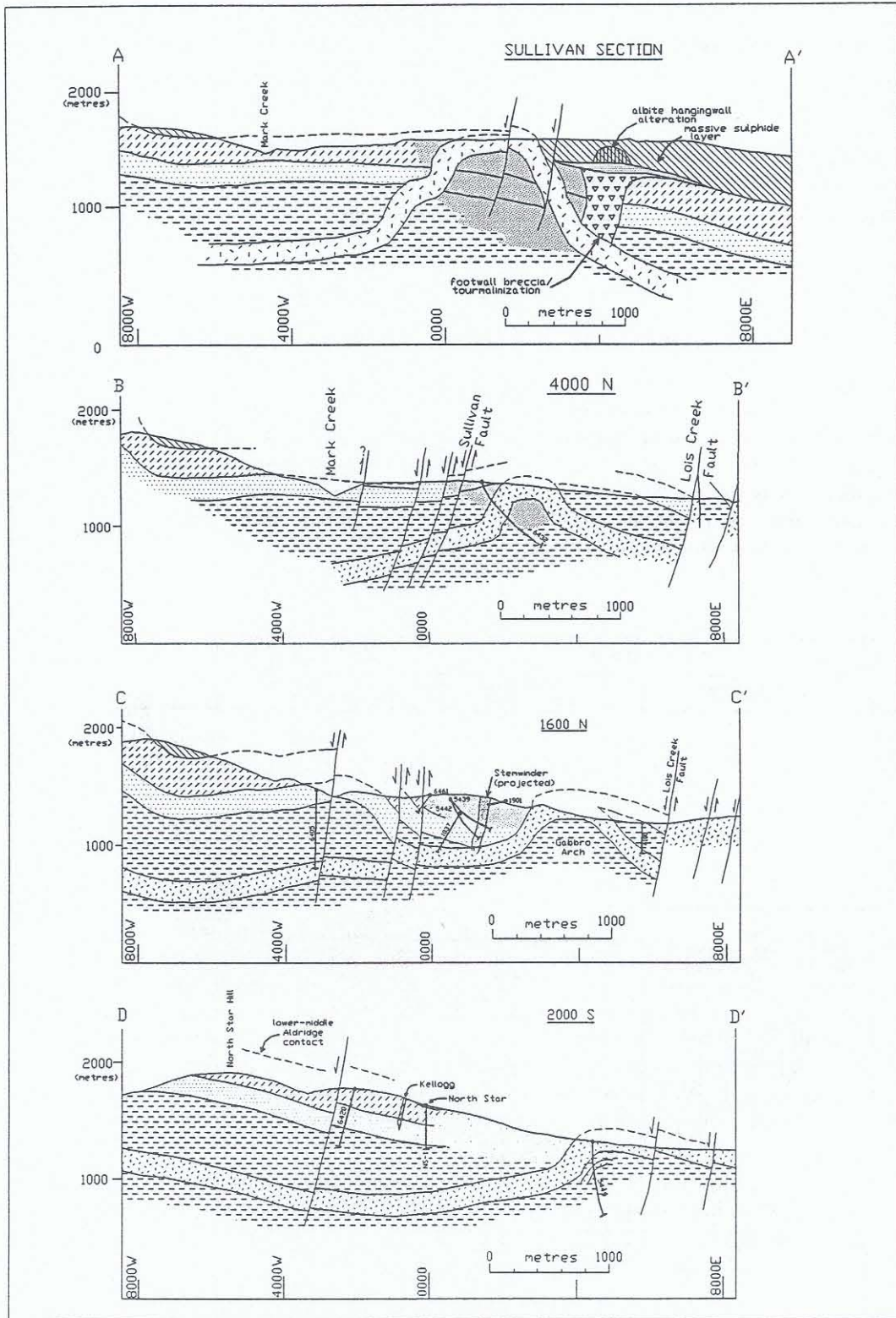


Figure 27. East-west geologic cross-sections of Sullivan - North Star trend (Höy, in press).

shallowest gabbro sill underlying the Sullivan orebody forms an anomalous arch along a NNW trend that is shallowly oblique to the trend of the alteration zone. Associated with the gabbro arch is an anomalous development of granophyre alteration of adjacent sediments. Within the alteration zone are five types of sulphide occurrence: (1) stratiform lead-zinc sulphides (Sullivan, North Star); (2) north-trending massive pyrrhotite ± Zn, Pb, Ag, Cu, Sn veins (Stemwinder, scattered small veins including some immediately underlying the Sullivan massive pyrrhotite body); (3) north trending quartz-chlorite-carbonate-pyrrhotite-pyrite-Zn-Pb-Ag veins (e.g. Quantrell, Midnight, Kellogg); (4) pyrrhotite vein stockwork (e.g. underlying Sullivan massive pyrrhotite body); and (5) dispersed and widespread disseminated and veinlet pyrrhotite ± Zn, Pb, Cu, Ag.

Return to intersection of Ross and Wallinger in downtown Kimberley.

### Start Point

**0.0 km** Ross St. and Wallinger St., Kimberley, B.C. Drive west on Ross St. following signs to Kimberley Ski area. Drive up switch backs, past Happy Hans Camp-ground. Stay left at fork to Purcell, Rocky Mountain and Silver Birch Condominium/chalets. Turn right onto road to ski lodge. Drive north on road to large parking area on north side of ski lodge complex.

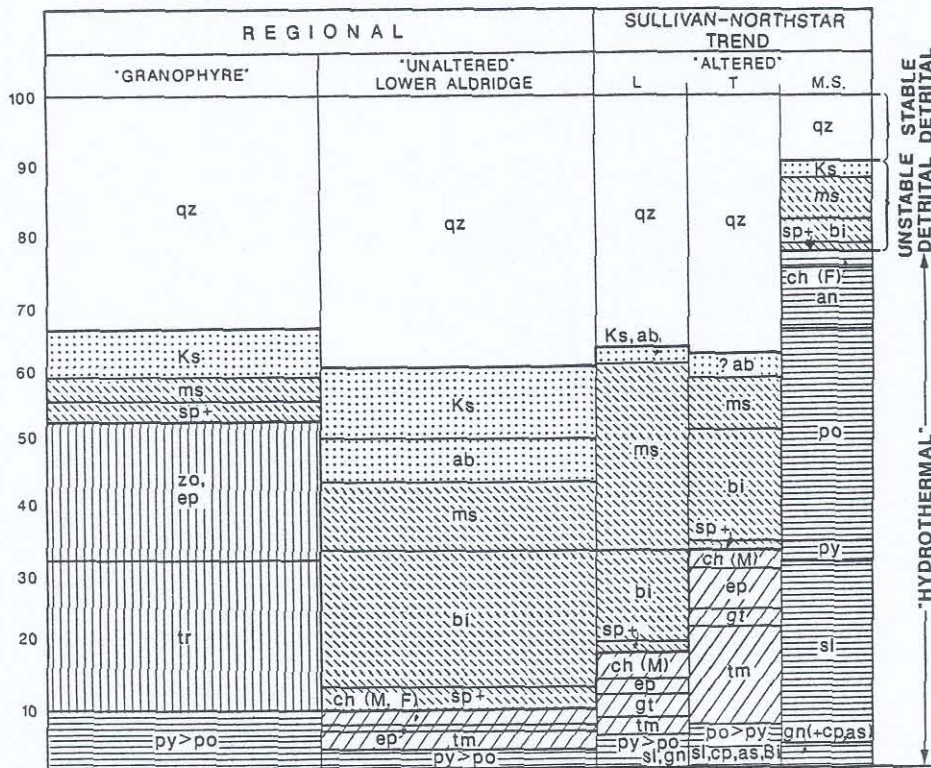


Figure 28. Schematic diagram of averaged modal mineralogy (abundances in per cent) for altered and unaltered rocks in the vicinity of Sullivan-North Star corridor. L = altered lower Aldridge, T = tourmalinite, M.S. = massive sulphide.

## STOP 2-5

### *SULLIVAN - NORTH STAR CORRIDOR (Turner, Leitch, Höy)*

Lower Aldridge feldspathic greywacke, siltite and argillite, within a zone extending 6 km south from and stratigraphically lower than the Sullivan orebody, are variably altered to muscovite-pyrite and tourmalinite assemblages which include variable quartz, muscovite, epidote, tourmaline, pyrite and pyrrhotite, lesser sphalerite and galena, and rare chalcopyrite and arsenopyrite (Figure 28; Leitch *et al.*, 1991). Metamorphic grade in these rocks is middle greenschist, as indicated by the assemblage quartz-muscovite-Mg chlorite-albite-microcline-biotite-epidote-garnet, whereas Fe-chlorite appears to be retrograde. Garnet, probably manganeseiferous, occurs only within altered rocks and likely reflects hydrothermal Mn enrichment of the original sediment. The presence of garnet provides an indicator of altered rocks, where other macroscopic criteria are lacking. Other more restricted exploration criteria such as abundant sulphides, tourmalinite and massive non-bedded or fragmental rocks can focus exploration within the garnet-bearing zone. Epidote-tremolite "granophyric" alteration is developed adjacent to Moyie sills.

Altered rocks in the Sullivan-North Star trend are distinguished from unaltered equivalents by the near absence of feldspars and the collective abundance of chlorite, epidote, garnet, tourmaline and sulphides (Fig. 28). The major minerals present in almost all samples (altered and unaltered) are quartz, muscovite and biotite. The only exceptions are a suite of (clino)zoisite-tremolite bearing rocks that may have undergone "granophyre" alteration near a Moyie sill west of the Sullivan-North Star trend and rocks where biotite has been converted to chlorite and/or muscovite.

Quartz grains, commonly 25  $\mu$ m to 0.2 mm size (silt to fine sand; rarely to 0.8 mm), retain their detrital size and shape with only minor overgrowths and suturing of boundaries. There is no clear evidence for addition of hydrothermal silica to altered rocks. The stable detrital character of quartz is shown by its almost constant abundance in all samples (until swamped by hydrothermal input in the massive sulphides of the North Star deposit: (Fig. 28). Muscovite most commonly occurs as abundant fine (50  $\mu$ m) subhedral flakes interstitial to the quartz grains, forming a matrix to them and locally imparting a weak to moderate foliation to the rock; minor coarse (0.1-0.5 mm) euhedral flakes are also scattered through the rock. Biotite is distinct by its occurrence as coarse (?porphyroblastic) 0.1-0.2 mm subhedral to euhedral books and flakes. It has deep brown pleochroism except where bleached or interleaved by muscovite and chlorite; aggregates of biotite and quartz locally create a "spotted" texture.

Feldspars (microcline and plagioclase) can form up to 20% of the unaltered rock, but are less abundant in altered rocks and massive sulphides, reflecting destruction/swamping by hydrothermal processes. In thin section, microcline has "grid" twinning and forms anhedral to subhedral, 25  $\mu$ m to 0.1 mm grains concentrated along bedding-parallel "sweat" veins grading to "clots", disseminated, on crosscutting fractures, or in some samples, euhedral laths of uncertain origin. Plagioclase is rarely identifiable, except where polysynthetic twinning is visible in coarser (0.1 mm) grains in bedding-parallel "sweats" or between quartz grains. Grains large enough for optical determination of composition are limited, but where observed are albite (An<sub>5-8</sub>). "Plagioclase" is differentiated from albite by a refractive index greater than quartz; where probed, it ranges from andesine (An<sub>38</sub>) in unaltered rocks to anorthite (An<sub>92</sub>) in partly tourmalinized rocks (Leitch, 1992b).

Detrital accessory minerals such as sphene, allanite, apatite, rutile, and carbonaceous matter also appear to be less abundant in altered rocks. Sphene, as subhedral grains up to 0.25 mm diameter, averages 3% in unaltered rocks but only 1% in altered rocks. Rutile, which replaces sphene and quartz as minute (10-25  $\mu$ m) euhedral needles, is more common in the altered rocks. Ilmenite forms subhedral grains up to 0.1 mm, commonly associated with sphene and pyrrhotite in the most altered rocks such as tourmalinite. However, at Sullivan sphene is part of the alteration assemblage (Leitch and Turner, 1991) and, along with apatite, is possibly remobilized rather than destroyed by alteration. Apatite forms clouded, euhedral prisms up to 50  $\mu$ m long in unaltered sediments but, as at Sullivan, in altered rocks it forms coarser (to

0.1 mm) clear subhedral grains. Carbon is found as minute (often  $\mu\text{m}$ ) grains interstitial to all other minerals, concentrated in layers in unaltered rocks but ?remobilized into round clots or balls in altered rocks; carbon abundances are slightly less in altered rocks. Zircon is difficult to identify due to similarity to allanite and sphene, but appears more common in altered rocks where it forms clear euhedral stubby prisms to 40  $\mu\text{m}$  long that lack pleochroic haloes in adjacent biotite or chlorite. Magnetite is not often identified in lower Aldridge rocks (however, Edmunds, 1977 describes magnetite associated with chloritization and carbonation).

Chlorite occurs mainly as a retrograde replacement of biotite. It forms subhedral flakes interleaved with muscovite and relict biotite, lacking the distinctive anomalous birefringence or pleochroism that would suggest an Fe-rich or magnesian composition. In a few cases, Fe-chlorite occurs as euhedral metacrysts up to 2 mm long. Minor Fe-chlorite with purple anomalous birefringence is associated with iron sulphides, particularly pyrite; this probably is a retrograde equilibration around the sulphides. This effect is also seen in radiation damaged haloes around allanite crystals (no monazite has yet been identified by SEM or probe studies; all the radioactive mineral grains investigated are allanite; cf. Schandl and Gorton, 1992).

Carbonate is more abundant in unaltered rocks, where it occurs as subhedral 0.25 mm grains that are mainly calcite or dolomite. In altered rocks it is absent; however, in massive sulphides it is present as inclusions of anhedral ankerite and ?siderite. Calcite or rarely dolomite with a similar habit, is present in Sullivan ore, possibly due to late chlorite-pyrite-calcite alteration (Hamilton *et al.*, 1983).

Chlorite in the "clots" or spots of alteration minerals is magnesian, forming coarse euhedral flakes up to 0.5 mm diameter similar to those seen in contact with the massive orebody at Sullivan (Leitch and Turner, 1991). Epidote abundance (1-3% in unaltered sediments) is clearly elevated in altered lower Aldridge rocks, especially in tourmalinite (7-13%). Epidote occurs principally in the clots of altered rocks, as subhedral grains up to 0.3 mm diameter lacking pleochroism, suggesting low Fe clinozoisite. Samples separated as "granophyre" in Figure 28 contain abundant zoisite (deep blue anomalous birefringence) and clinozoisite as subhedral crystals up to 0.5 mm, plus tremolite as bladed laths up to 1 mm long in a distinctive assemblage that has a more recrystallized texture than the majority of sediments studied. These samples lie well outside the Sullivan-North Star trend, but may be part of wet sediment alteration related to intrusion of nearby Moyie sills (cf. Höy, 1989).

Garnet is present in almost all altered lower Aldridge samples from within the Sullivan-North Star trend but absent from the samples studied from outside the trend. Garnets in unaltered Aldridge metasediments are not common elsewhere (Edmunds, 1977). However they do occur locally in some samples from the core of the Moyie anticline near the St. Eugene mine. Garnet is also absent from samples close to or overlying the Sullivan orebody. Garnets occur as euhedral crystals up to 2 mm diameter with sieve texture due to inclusions of quartz, and less commonly as anhedral masses in bed-parallel veins. Garnets are manganiferous (to 22% MnO; Leitch, 1992b).

Tourmaline has two distinct forms in the altered rocks: (1) 1-5% coarse (up to 0.4 mm) euhedral prisms of greenish-brown to slate-blue (Fe-rich), or lesser yellow-brown (Mg-rich) intermediate dravite-schorl (Leitch, 1992b), and (2) up to 25% extremely fine (5-15  $\mu\text{m}$ ), felted pale greenish needles also intermediate in composition between schorl and dravite (Ethier and Campbell, 1977). Fine-grained tourmaline replaces feldspar grains interstitial to the detrital quartz as well as the margins and some centers of other minerals, including quartz, biotite, garnet and epidote. The coarse tourmaline is similar to detrital schorl present in unaltered sediments. Fine-grained tourmaline characterizes the tourmalinite samples and reflects hydrothermal alteration.

Sulphide abundance increases progressively from unaltered rock to altered rock to tourmalinite to massive sulphide. The variety of base metal sulphides increases with increasing sulphide abundance such that assemblages include not only sphalerite but also galena, chalcopyrite, and finally arsenopyrite (and rare native Bi). Pyrite, as euhedral cubes to 0.5 mm across, is generally more abundant than pyrrhotite, except in tourmalinite, where pyrrhotite

is dominant. Pyrrhotite forms subhedral aggregates of 0.25 mm grains; it is commonly oxidized to lamellar marcasite-pyrite. All Fe-sulphides in surface samples show some replacement by limonite. Sphalerite, with red-brown colour indicating moderate Fe content similar to that at Sullivan, and galena form subhedral to anhedral grains up to 0.35 mm across. Chalcopyrite and arsenopyrite occur as minor anhedral blebs and euhedral rhombs respectively, up to 0.1 mm across, within the other sulfides; minute (25 m) rounded blebs of possible native Bi (Leitch, 1992b) are rare.

Return to intersection of Ross and Wallinger in downtown Kimberley.

- 0.0 km** Traffic lights at intersection of Ross St. and Wallinger St., Kimberley, B.C. Drive south on Wallinger (Highway 95A), which becomes Warren St.
- 5.8 km** Turn right (west) on St. Mary Lake Road. Road climbs thick glacial deposits. Pit at top of hill exposes east-dipping forset beds in Pliostocene gravels.
- 9.5 km** Kimberley city limits
- 10.8 km** **ALTERED GABBRO-SEDIMENT CONTACT** Low outcrops on right (north) side of road expose contact between gabbro and lower Aldridge interbedded siltstone and argillite. A thin zone of albitized sedimentary rock occurs along the lower gabbro contact. The upper contact is obscured by coarse biotite-quartz-feldspar alteration of sediment and chlorite-amphibole alteration of gabbro.

## STOP 2-6

### 0.0 km *VIEW OF GABBRO SILL COMPLEX, LOWER ALDRIDGE FORMATION, BOOTLEG MOUNTAIN, ST. MARY VALLEY* (Turner, Höy and Anderson)

Park along west side of road below "Y" junction. Walk back 50 m to junction of track on east side that runs east into clearcut. There is a good view to the north from the

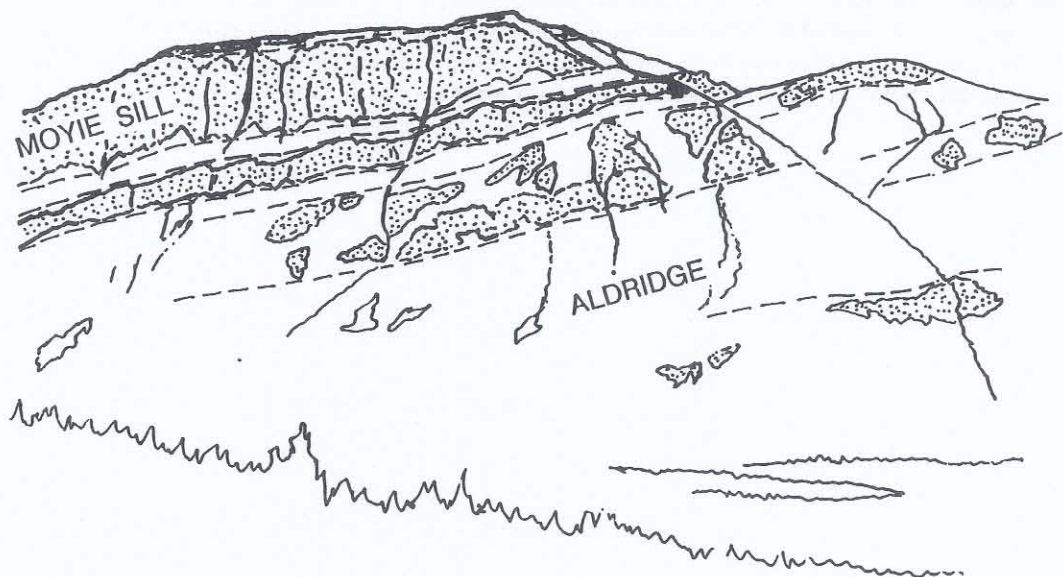


Figure 29. Sketch of gabbro sill complex in lower Aldridge Formation, Bootleg Mountain (Stop 2-6).

clearcut area. Bootleg Mountain, the dominant peak to the north, exposes about 3000 metres of lower Aldridge strata intruded by the gabbro sill complex. The stratigraphic level of the Sullivan horizon is about 2000 m above the uppermost sill exposed (Figure 29). The aggregate thickness of gabbro exposed in this section is estimated as 1000 m within a sequence 3000 m thick. The base of the section is not exposed; to the east in the valley of Mathew Creek, the lower Aldridge is metamorphosed to sillimanite-garnet-bearing quartz-mica schists. Metamorphism is interpreted as coeval with folds and cleavage cut by the HellRoaring Creek stock (Leech, 1958), dated as 1340 Ma (Ryan and Blenkinsop, 1971). This Proterozoic deformation is named East Kootenay Orogeny by MecMechan and Price (1982). The lower Aldridge section is juxtaposed against the higher grade metamorphic rocks along a mylonitic fault zone (P. Ransom, personal communication).

## Comment

The large volume of gabbro sills in the stratigraphic interval underlying the Sullivan deposit begs the question as to the role of sill emplacement in ore formation and rock alteration. Leech (1958) recognized two sets of gabbro sills in the St. Mary valley. The lower sill complex occurs throughout the exposed 3000 m of lower Aldridge strata and has an aggregate thickness of 1000 metres; a lower cluster of sills in Aldridge strata are also well exposed southwest of the Sullivan mine (Leech, 1957). The stratigraphically highest sills in the complex are just below the contact with the overlying middle Aldridge Formation, the stratigraphic level of the Sullivan orebody. A second, smaller sill complex occurs near the middle of the middle Aldridge Formation.

Höy (1989) suggested that the Moyie sills were intruded into unconsolidated Aldridge sediment and proposed the Guaymas sedimented rift basin as a modern analogy. Basalt sill complexes are known to intrude modern sediments to within tens of meters of the present seafloor (Einsele, 1982; Gieskes *et al.*, 1982). A model for intrusion by Einsele (1982) assumes upward-younging sills as each subsequent magma injection rises to the top of previously altered sediment, achieves neutral bouyancy and spreads laterally. Such sills are only slightly younger than the sediments they intrude. One might speculate therefore, that the minimum age of the two gabbro sill complexes exposed southwest of the Sullivan mine (Leech, 1957) can be dated by the stratigraphic level of the uppermost sill of each complex: an older intrusive event up to the time of formation of the Sullivan deposit, and a younger event during middle Aldridge time. Such a scenario raises the larger question of the role of the source magma for the Moyie sills as a heat engine of fluids that formed the Sullivan orebody, as suggested by Hamilton (1984).

# BIBLIOGRAPHY

- Ansdell, K.M., Nesbitt, B.D. and Longstaffe, F.J. (1989): A Fluid Inclusion and Stable Isotope Study of the Tom Ba-Pb-Zn Deposit, Yukon Territory, Canada; *Economic Geology*, v. 84, p.841-856.
- Baumgartner, T.R., Ferreira-Bartrina, V. and Moreno-Hentz, P. (1991): Varve Formation in the Central Gulf of California: A Reconsideration of the Origin of the Dark Laminac from the 20th Century Varve Record; in: J.P. Dauphin and B.R.T. Simoneit (Editors), *The Gulf and Peninsular Province of the Californias*; *American Association Petroleum Geologists Memoir* 47., p. 617-635.
- Beaty, D.W., Hahn, G.A. and Threlkeld, W.E. (1988): Field, Isotopic and Chemical Studies of Tourmaline-bearing Rocks in the Belt - Purcell Supergroup: Genetic Constraints and Exploration Significance for Sullivan Type Ore Deposits; *Canadian Journal of Earth Science*, v. 25, p.392-402.
- Benvenuto, G.L. and Price, R.A. (1979): Structural Evolution of the Hosmer Thrust Sheet, Southeastern British Columbia, *Bulletin of Canadian Petroleum Geologists*, v. 27, p.360-394.
- Bishop, D.T. (1974b): Petrology and Geochemistry of the Purcell Sills in Boundary County, Idaho, in Belt Symposium, Volume II, *Department of Geology, University of Idaho and Idaho Bureau of Mines and Geology*, p. 15 -66.
- Boles, J.R. (1982): Active Albitization of Plagioclase, Gulf Coast Tertiary; *American Journal of Science*, v. 292, p. 165-180.
- Bouma, A.H. (1962): Sedimentology of some Flysch Deposits, *Elsevier Publishing Co.*, Amsterdam, 168 pages.
- Carter, G. and Höy, T. (1987a): Geology of the Skookumchuck Map Area, Southeastern British Columbia, B.C. Ministry of Energy, Mines and Petroleum Resources, Geological Fieldwork 1986, Paper 1987-1, p. 143-156.
- Carter, G. and Höy, T. (1987b): Geology of the Skookumchuck Map Area (W1/2), Southeastern British Columbia, B.C. Ministry of Energy, Mines and Petroleum Resources, Open File 1987-8.
- Deiss, C. (1941): Cambrian Geography and Sedimentation in the Central Cordilleran Region, *Geological Society of America*, Bulletin 52, p. 1085-1116.
- Devlin, W.J. and Bond, G.C. (1988): The Initiation of the Early Paleozoic Cordilleran Miogeocline: Evidence from the Uppermost Proterozoic - Lower Cambrian Hamill Group of Southeastern British Columbia, *Canadian Journal of Earth Sciences*, Volume 25, p. 1-19.
- Edmunds, F.R. (1977): Kimberley to Creston, Stratigraphy and Lithology of the Lower Belt Series in the Purcell Mountains, British Columbia, in Höy, T., (editor) *Lead- Zinc Deposits of Southeastern British Columbia*, *Geological Association of Canada Fieldtrip Guidebook* 1, p. 22-32.
- Edmunds, F.R. (1977): The Aldridge Formation, B.C., Canada; Ph.D. thesis, *Pennsylvania State University*, University Park, Pennsylvania, 368 p.
- Einsele, G. (1982): Mechanism of Sill Intrusion into Soft Sediment and Expulsion of Pore Water, in *Initial Reports of the Deep Sea Drilling Project*, Volume LXIV, Part 2, p. 1169-1176.
- Ethier, V.G., Campbell, F.A., Both, R.A. and Krouse, H.R. (1976): Geological Setting of the Sullivan Orebody and Estimates of Temperatures and Pressure of Metamorphism, *Economic Geology*, Volume 71, p. 1570-1588.
- Ethier, V.G. and Campbell, F.A. (1977): Tourmaline Concentrations in Proterozoic Sediments of the Southern Cordillera of Canada and their Economic Significance; *Canadian Journal of Earth Science*, v. 14, p. 2348-2363.
- Freeze, A.C. (1966): On the Origin of the Sullivan Orebody, Kimberley, B.C., in *Tectonic History and Mineral Deposits of the Western Cordillera*; *Canadian Institute of Mining and Metallurgy*, Special Volume 8, p. 263-294.
- Gardner, H.D. and Hutcheon, I. (1985): Geochemistry, Mineralogy and Geology of the Jason Pb-Zn Deposits, MacMillan Pass, Yukon, Canada; *Economic Geology*, v. 80, p.1257-1276.
- Goodfellow, W.D. and Rhodes, D. (1990): Geological Setting, Geochemistry and Origin of the Tom Zn-Pb-Ag-barite Deposits, in Abbot, J.G. and Turner, R.J.W. (editors), *Mineral Deposits of the Northern Canadian Cordillera, Yukon-northeastern British Columbia*, IAGOD Field Guide, Excursion 14; *Geological Survey of Canada*, Open File 2169, p.177-241.

- Gwosdz, W. and Krebs, W. (1977): Manganese Halo Surrounding Meggen Ore Deposit, Germany; *Transactions Institution of Mining and Metallurgy* (Sect. B: Applied earth science), v. 86, p. 73-77.
- Hagen, A.S. (1985): Fragmentals in the Sullivan-North Star Corridor; Unpublished Report, *Cominco Ltd.*, 10 pages.
- Hagen, A.S., Hamilton, J.M., Ransom, P.W. and Owens, O.E. (1989): Solving the Kimberley Fault Problem and Location of the Faulted Off Part of the Sullivan Orebody (Abstract); in Evolution of Proterozoic Rocks of the Northern Cordillera, *Geological Society of America, Rocky Mountain and Cordilleran Sections Annual Meeting*, Spokane, Washington.
- Hamilton, J.M. (1984): The Sullivan Deposit, Kimberley, British Columbia - a Magmatic Component to Genesis? (abstract), in The Belt, Belt symposium II, *Montana Bureau of Mines and Geology*, Special Publication 90, p. 58-60.
- Hamilton, J.M. and Balla, J. (1983): Belt-Purcell Supergroup; Troy (Spar Lake), in Höy et al., 1985, Stratabound Base Metal Deposits in Southeastern British Columbia and Northwestern Montana, *Geological Association of Canada*, Field Trip 11, p. 25-31.
- Hamilton, J.M., Bishop, D.T., Morris, H.C., Owens, O.E. (1982): Geology of the Sullivan Orebody, Kimberley, B.C., Canada, in Precambrian Sulphide Deposits, H.S. Robinson Memorial Volume; R.W. Hutchinson, C.D. Spence and J.M. Franklin (editors) *Geological Association of Canada*, Special Paper 25, p. 597-665.
- Hamilton, J.M., Delaney, G.D., Hauser, R.L. and Ransom, P.W. (1983): Geology of the Sullivan Deposit, Kimberley, B.C., in Sediment-hosted Stratiform Lead-zinc Deposits; D.F. Sangster, (editor), *Mineralogical Association of Canada*, Short Course Notes, Chapter 2, p. 31-83.
- Harrison, J.E. (1972): Precambrian Belt Basin of Northwestern United States: Its Geometry, Sedimentation and Copper Occurrences, *Geological Society of America*, Bulletin, Volume 83, p. 1215-1240.
- Harrison, J.E., Griggs, A.B. and Wills, J.D. (1974): Tectonic Features of the Precambrian Belt Basin and their Influence on Post-Belt Structures, *United States Geological Survey*, Professional Paper 866.
- Hay, B.J. and Honjo, S. (1989): Particle Deposition in the Present and Holocene Black Sea, *Oceanography*, v. 2, p. 26-31.
- Heubschman, R.P. (1973): Correlation of Fine Carbonaceous Bands Across a Precambrian Stagnant Basin, *Journal of Sedimentary Petrology*, Volume 43, p. 688-699.
- Hoffman, P.F. (1991): Did the Breakout of Laurentia Turn Gondwanaland Inside-out?; *Science*, v. 252, p. 1409-1412.
- Höy, T. (1979): Geology of the Estella-Kootenay King Area, Hughes Range, Southeastern British Columbia, *B.C. Ministry of Energy, Mines and Petroleum Resources*, Preliminary Map 36.
- Höy, T. (1982): The Purcell Supergroup in Southeastern British Columbia; Sedimentation, Tectonics and Stratiform Lead-Zinc Deposits, in Precambrian Sulphide Deposits, H.S. Robinson Memorial Volume; R.W. Hutchinson, C.W. Spence and J.M. Franklin, (Editors) *Geological Association of Canada*, Special Paper 25, p. 127-147.
- Höy, T. (1984a): Structural Setting, Mineral Deposits and Associated Alteration and Magmatism, Sullivan Camp, Southeastern British Columbia, *Geological Fieldwork 1983*, *B.C. Ministry of Energy, Mines and Petroleum Resources*, Paper 1984-1, p. 24-35.
- Höy, T. (1984b): Geology of the Cranbrook Sheet and Sullivan Map Area, *B.C. Ministry of Energy, Mines and Petroleum Resources*, Preliminary Map 54.
- Höy, T. (1989): The Age, Chemistry and Tectonic Setting of the Middle Proterozoic Moyie Sills, Purcell Supergroup, Southeastern British Columbia, *Canadian Journal of Earth Sciences*, Volume 29, p. 2305-2317.
- Höy, T. (in press): Geology of the Purcell Supergroup in the Fernie West-half Map-area, Southeastern British Columbia, *B.C. Ministry of Energy, Mines and Petroleum Resources*, Bulletin 84.
- Höy, T., Berg, N., Fyles, J.T., Delaney, G.D., McMurdo, D. and Ransom, P.W. (1985): Stratabound Base Metal Deposits in Southeastern British Columbia, Field Trip 11, in Field Guides to Geology and Mineral Deposits in Southern Canadian Cordillera, *Geological Association of Canada*, D. Tempelman-Kluit, (editor), 32 pages.
- Höy, T. and Carter, G. (1988): Geology of the Fernie West Half Map Sheet (and Part of Nelson East-Half), *B.C. Ministry of Energy, Mines and Petroleum Resources*, Open File Map 1988-14.
- Höy, T. and Diakow, L. (1982): Geology of the Moyie Lake Area, *B.C. Ministry of Energy, Mines and Petroleum Resources*, Preliminary Map 49.
- Hunt, G. (1962): Time of Purcell Eruption in Southeastern British Columbia and Southwestern Alberta, *Journal of the Alberta Society of Petroleum geologists*, Volume 10, p. 438-442.

- Jardine, D.E. (1966): An Investigation of Brecciation Associated with the Sullivan Mine Orebody at Kimberley, B.C., Unpublished M.Sc. Thesis, *University of Manitoba*, Winnipeg, Manitoba.
- Kanasewich, E.R. (1968): Precambrian Rift: Genesis of Stratabound Ore Deposits, *Science*, Volume 161, pages 1002-1005.
- Kanasewich, E.R., Clowes, R.M. and McCloughan, C.H. (1969): A Buried Precambrian Rift in Western Canada, *Tectonophysics*, Volume 78, p. 513-527.
- LeCouteur, P.C. (1979): Age of the Sullivan Lead-Zinc Deposit (Abstract), *Geological Association of Canada*, Cordilleran Section, Program with Abstracts, page 19.
- Leech, G.B. (1957): St. Mary Lake, Kootenay District, British Columbia (82F/9), *Geological Survey of Canada*, Map 15-1957.
- Leech, G.B. (1960): Geology Fernie (West Half), Kootenay District, British Columbia, *Geological Survey of Canada*, Map 11-1960.
- Leitch, C.H.B. (1992a): A Progress Report of Fluid Inclusion Studies of Veins from the Vent Zone, Sullivan Stratiform Sediment-hosted Zn-Pb Deposit, British Columbia; in Current Research, Part E, *Geological Survey of Canada*, Paper 92-1E, p. 71-82.
- Leitch, C.H.B. (1992b): Mineral Chemistry of Selected Silicates, Carbonates and Sulphides in the Sullivan and North Star Stratiform Zn-Pb Deposits, British Columbia and in District-scale Altered and Unaltered Sediments; in Current Research, Part E, *Geological Survey of Canada*, Paper 92-1E, p. 83-93.
- Leitch, C.H.B. and Turner, R.J.W. (1991): The Vent Complex of the Sullivan Stratiform Sediment-hosted Zn-Pb Deposit, B.C.: Preliminary Petrographic and Fluid Inclusion Studies; in Current Research, Part E, *Geological Survey of Canada*, Paper 91-1E, p. 33-44.
- Leitch, C.H.B. and Turner, R.J.W. (1992): Sulphide-Bearing Network Underlying the Western Orebody, Sullivan Stratiform Sediment-hosted Zn-Pb Deposit, B.C.: Preliminary Field, Petrographic and Fluid Inclusion Studies; in Current Research, Part E, *Geological Survey of Canada*, Paper 92-1E (this volume).
- Leitch, C.H.B., Turner, R.J.W. and Höy, T. (1991): The District-scale Sullivan-North Star Alteration zone, Sullivan Mine area, British Columbia: a Preliminary Petrographic Study; in Current Research, Part B, *Geological Survey of Canada*, Paper 91-1E, p.45-57.
- Leitch, C.H.B., Turner, R.J.W. and Höy, T. (1991): The District-Scale Sullivan-North Star Alteration Zone, Sullivan Mine Area, B.C.: A Preliminary Petrographic Study, *Geological Survey of Canada*, Report of Activities.
- Lis, M.G. and Price, R.A. (1976): Large-Scale Block Faulting During Deposition of the Windermere Supergroup (Hadrynian) in Southeastern British Columbia, *Geological Survey of Canada*, Paper 1976-1A, p. 135-136.
- Luternauer, J.L., Clague, J.J. and Pharo, C.H. (1983): Substrates of the Strait of Georgia, British Columbia; *Canadian Journal of Fisheries and Aquatic Sciences*, v. 40, p. 1026-1032.
- Mako, D.A. and Shanks, W.C. III. (1984): Stratiform Sulfide and Barite-fluorite Mineralization of the Vulcan Prospect, Northwest Territories: Exhalation of Basinal Brines Along a Faulted Continental Margin; *Canadian Journal of Earth Sciences*, v. 21, p.78-91.
- McAdam, J.H. (1978): A Preliminary Study of Footwall Mineralization at the Sullivan mine, Kimberley, B.C.; B.Sc. Thesis, *Queen's University*, Kingston, 71 p.
- McClay, K.R. (1983): Structural Evolution of the Sullivan Fe-Pb-Zn-Ag Orebody, Kimberley, British Columbia, Canada, *Economic Geology*, Volume 78, p. 1398-1424.
- McDougall, J. (1984): Fluid Dynamic Implications for Massive Sulphide Deposits Flowing into a Submarine Depression from Below; *Deep Sea Research*, v.2, p.145-170.
- McMechan, M.E. (1979): Geology of the Mount Fisher-Sand Creek area, B.C. *Ministry of Energy, Mines and Petroleum Resources*, Preliminary Map 34.
- McMechan, M.E. (1981): The Middle Proterozoic Purcell Supergroup in the Southwestern Purcell Mountains, British Columbia and the Initiation of the Cordilleran Miogeocline, Southern Canada and Adjacent United States, *Bulletin of Canadian Petroleum Geology*, Volume 29, p. 583-621.
- McMechan, M.E. and Price, R.A. (1982): Superimposed Low -Grade Metamorphism in the Mount Fisher Area, Southeastern British Columbia - Implications for the East Kootenay Orogeny, *Canadian Journal of Earth Sciences*, Volume 19, p. 476-489.
- Nesbitt, B.E. (1986): Oxide-sulfide-silicate Equilibria Associated with Metamorphosed Ore Deposits. Part II: Pelitic and Felsic Volcanic Terrains; *Economic Geology*, v. 81, p. 841-856.
- Nesbitt, B.E., Longstaffe, F.J. and Muehlenbachs, K., (1984): Oxygen Isotopic Geochemistry of the Sullivan Massive Sulfide Deposit, Kimberley, British Columbia; *Economic Geology*, v. 79, p.933-946.

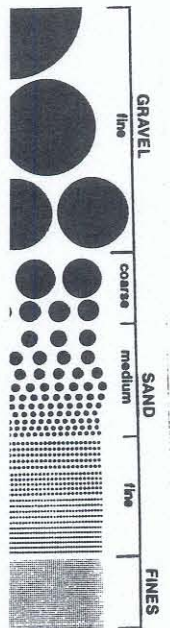
- Obradovich, J.D. (1973): A Review of the Geochronology of Belt and Purcell Rocks, in Belt Symposium, Volume 1, *Department of Geology, University of Idaho and Idaho Bureau of Mines and Geology*, p. 8-9.
- Obradovich, J.D., Zartman, R.E. and Peterman, Z.E. (1984): Update of the Geochronology of the Belt Supergroup, in The Belt, S.W. Hobbs (Editor) *Montana Bureau of Mines and Geology, Special Publication 90*, p. 82-84.
- Parrish, R.R., Carr, S.D. and Parkinson, D.L. (1988): Eocene Extensional Tectonics and Geochronology of the Southern Omineca Belt, British Columbia and Washington, *Tectonics*, Volume 7, p. 181-212.
- Pighan, D.L. (1983): St. Joe property, 1982 year end report; Cominco Ltd., unpublished report, 10 pages.
- Price, R.A. (1962): Fernie Map-area, East-half, Alberta and British Columbia, *Geological Survey of Canada*, Paper 61-24.
- Price, R.A. (1964): The Precambrian Purcell System in the Rocky Mountains of Southern Alberta and British Columbia, *Bulletin of Canadian Petroleum Geology*, Volume 12, p. 399-426.
- Price, R.A. (1981): The Cordilleran Foreland Thrust and Fold Belt in the Southern Canadian Cordillera, in Thrust and Nappe Tectonics, K.R. McClay and N.J. Price (Editors); *Geological Society of London*, Special Publication 9, p. 427-448.
- Ramboz, C., Oudin, E. and Thisse, Y. (1988): Geysier-type Discharge in Atlantis II deep, Red Sea: Evidence of Boiling from Fluid Inclusions in Epigenetic Anhydrite; *Canadian Mineralogist*, v. 26, p. 765-786.
- Ransom, P.W., Delaney, G.D. and McMurdo, D. (1985): The Sullivan Orebody, in Höy *et al.*, 1985, Stratabound Base Metal Deposits in British Columbia, *Geological Association of Canada, Field Trip 11*, p. 20-28.
- Reesor, J.E. (1973): Geology of the Lardeau Map-area, East-half, British Columbia, *Geological Survey of Canada*, Memoir 369, 129 pages.
- Reesor, J.E. (1983): Geology of the Nelson Map-area, East-half, *Geological Survey of Canada*, Open File 929.
- Rice, H.M.A. (1937): Cranbrook Map-area, British Columbia, *Geological Survey of Canada*, Memoir 207.
- Ross, G.M., (1992): The Origin of the Pacific Ocean. *Water On Earth*, v. 5, p. 24-25.
- Russell, M.J. (1974): Manganese Halo Surrounding the Tynagh Ore Deposit, Ireland: a Preliminary Note; *Transactions Institution of Mining and Metallurgy* (Sect. B: Applied earth science), v. 83, p. 65-66.
- Ryan, B.D. and Blenkinsop, J. (1971): Geology and Geochronology of the Hellroaring Creek Stock, British Columbia, *Canadian Journal of Earth Sciences*, Volume 8, p. 85-95.
- Samson, I.M. and Russell, M.J. (1983): Fluid Inclusion Data from Silvermines Base-metal - baryte Deposits, Ireland; *Transactions of the Institution of Mining and Metallurgy* (Section B: Applied earth science), v. 92, p.67-71.
- Schandl, E.S. and Gorton, M.P. (1992): Rare-earth Element Geochemistry of Selected Samples from the Sullivan Pb-Zn Sedex Deposit: the Role of Allanite in Mobilizing Rare-earth Elements in the Chlorite-rich Footwall (82G/12); in Geological Fieldwork, 1991, *British Columbia Ministry of Energy, Mines and Petroleum Resources*, Paper 1992-1, p. 273-279.
- Schofield, S.J. (1915): Geology of the Cranbrook Area, *Geological Survey of Canada*, Memoir 76, 245 pages.
- Sears, J.W. and Price, R.A. (1978): The Siberian Connection: a Case for Precambrian Separation of the North American and Siberian Cratons, *Geology*, Volume 6, p. 267-270.
- Shaw, D.R. and Hodgson, C.J. (1980): Wall-rock Alteration at the Sullivan Mine, Kimberley, British Columbia (abstract), 5th Annual *Canadian Institute of Mining*, District 6 Convention, Kimberley, B.C., Program and Abstracts.
- Shaw, D.R. and Hodgson, C.J. (1986): Wall-rock Alteration at the Sullivan Mine, Kimberley, B.C., in The Genesis of Stratiform Sediment-hosted Lead and Zinc Deposits: Conference Proceedings, R.J.W. Turner and M.T. Einaudi (editors); *Stanford University Publications, School of Earth Sciences*, v. XX, p.13-21.
- Taylor, B.E. and Slack, J.F. (1984): Tourmalines from Appalachian-Caledonia Massive Sulfide Deposits: Textural, Chemical and Isotopic Relationships; *Economic Geology*, v. 79, p. 1703-1726.
- Turner, R.J.W. (1990): Jason Stratiform Zn-Pb-barite Deposit, Selwyn Basin, Canada (NTS 105-O-1): Geological Setting, Hydrothermal Facies and Genesis, in Abbot, J.G. and Turner, R.J.W. (editors), Mineral Deposits of the Northern Canadian Cordillera, Yukon-northeastern British Columbia, IAGOD Field Guide, Excursion 14; *Geological Survey of Canada*, Open File 2169, p.137-175.

- Turner, R.J.W. and Leitch, C.H.B. (1992): Relationship of Albitic and Chloritic Alteration to Gabbro Dikes and Sills in the Sullivan Mine and Nearby Area, B.C.; in Current Research, Part E, *Geological Survey of Canada*, Paper 92-1E, p. 95-105.
- Winston, D. (1986a): Sedimentation and Tectonics of the Middle Proterozoic Belt Basin and their Influence on Phanerozoic Compression and Extension in Western Montana and Northern Idaho, in Paleotectonics and Sedimentation in the Rocky Mountain region, United States, Peterson, J. (Editor) *American Association of Petroleum Geologists*, Memoir, Part II, p. 87-118.
- Winston, D. (1986b): Stratigraphic Correlation and Nomenclature of the Middle Proterozoic Belt Supergroup, Montana, Idaho and Washington, in Belt Supergroup: a Guide to Proterozoic Rocks of Western Montana and Adjacent Areas, S. Roberts (Editor) *Montana Bureau of Mines and Geology*, Special Publication 94.
- Winston, D., Woods, M. and Byer, G.B. (1984): The Case for an Intracratonic Belt-Purcell Basin: Tectonic, Stratigraphic and Stable Isotope Considerations, Montana, *Geological Society of America*, 1984 Field Conference, p. 103-118.
- Zartman, R.E., Peterman, Z.E., Obradovich, J.D., Gellego, M.D. and Bishop, D.T. (1982): Age of the Crossport C Sill near Eastport, Idaho, in Coeur d'Alene Field Conference, R.R. Reid and G.A. Williams (Editors), *Idaho Society of Economic Geologists, Bureau of Mines and Geology*, Bulletin 24, p. 61-69.
- Zierenberg, R.A. and Shanks, W.C.III. (1988): Isotopic Studies of Epigenetic Features in Metalliferous Sediment, Atlantis II Deep, Red Sea; *Canadian Mineralogist*, v. 26, p. 737-753.

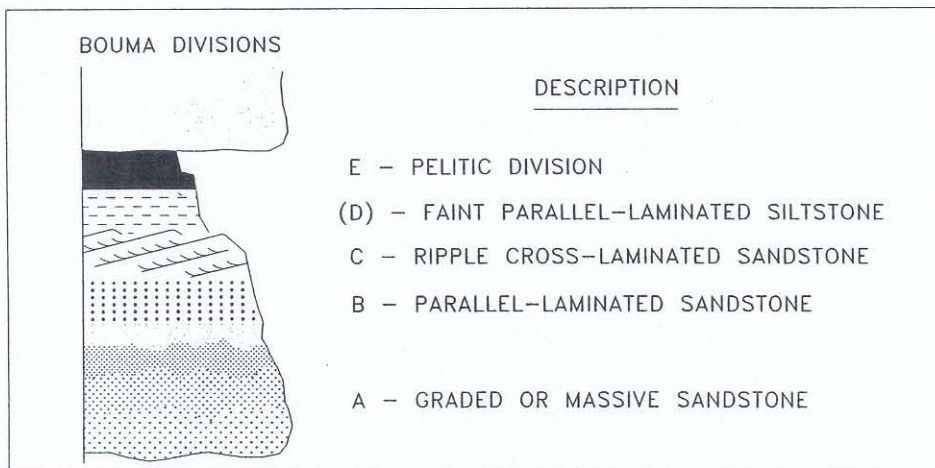
***Notes***

---

Notes



CENTIMETRE



# GEOLOGIC TIME SCALE - BRITISH COLUMBIA GEOLOGICAL SURVEY BRANCH



Phanerozoic data derived from:  
 1) W.B.Harland et al. (1990)  
 PreCambrian data from:  
 1) Lumbers & Card (Geology, Vol. 20 1991)

PERIOD		CENOZOIC			MESOZOIC			PALEOZOIC			EON						
		Epoch / Stage	Ma Age	Period	Epoch / Stage	Ma Age	Period	Period	Epoch / Stage	Ma Age	ERA	PERIOD	Ma Age				
QUATERNARY	Holocene	Calabrian	0.01	Cretaceous	Maastrichtian	65.0 ± 2	PERMIAN	Late	Changhsingian	245 ± 9.5	PROTEROZOIC	Neoproterozoic	570				
		Piacenzian	1.64		Campanian	74.0 ± 3		Early	Changhsingian	247.5 ± 11							
	PLIOGENE	Zanclean	3.40 ± 1.35	Cretaceous	Santonian	83 ± 4	PENNSYLVANIAN	Early	Artinskian	269 ± 11			Neoproterozoic	Neoproterozoic III	650		
		Messinian	5.2 ± 1.5 6.7 ± 2.3		Turonian	86.6 ± 3 88.5 ± 2 90.4 ± 2			MOSCOWIAN	Sakmarian						281.5 ± 1.3	
	NEOGENE	Tortonian	10.4 ± 1.5	Cretaceous	Cenomanian	97.0 ± 2	MISSISSIPPIAN	Late		Kasimovian			290 ± 9 295 ± 6.5 303 ± 5	Mesoproterozoic	Mesoproterozoic	1000	
		MIOCENE	Serravallian		14.2 ± 1.8	Albion		Albion	Early	Bashkirian			311.5 ± 9.5				
			Langhian		16.3 ± 1					Barremian			112 ± 2				Serpukhovian
	PALEOGENE	Eocene	Burdigalian	21.5 ± 1.8	Cretaceous	Barremian	124.5 ± 1.3	DEVONIAN	Early	Tournaisian			349.5 ± 4.5	ARCHEAN	Mesoproterozoic	1200	
			Rupelian	23.3 ± 1		Hauterivian	131.8 ± 8 135.0 ± 8		MIDDLE	Famennian			362.5 ± 5.5 367 ± 5				
		Oligocene	Aquitanian	21.5 ± 1.8	Valanginian	140.7 ± 1.3	EARLY	Frasnian		377.5 ± 10			Paleoproterozoic				Paleoproterozoic
Chattian			28.3 ± 1.5	Berriasian	145.6 ± 9.5	Middle		Givetian	381 ± 11								
TERTIARY		Eocene	Chattian	28.3 ± 1.5	Cretaceous	Tithonian	152.1 ± 11.5	SILURIAN	Late	Ludlovian	424 ± 4	Neoproterozoic	Neoproterozoic				1600
			Rupelian	23.3 ± 1		Kimmeridgian	154.7 ± 6.5		LATE	Eifelian	386 ± 5.3 390.5 ± 12						
		Oligocene	Chattian	28.3 ± 1.5	Oxfordian	157.1 ± 8	EARLY	Siegeminian/Pragian		464 ± 7.5							
			Priabonian	35.4 ± 1.4	Collovian	161.3 ± 7		MIDDLE	Gedinnian/Lochkovian	467 ± 7.5 473 ± 7.5							
Eocene		Bartonian	38.6 ± 1.5	Bathonian	166.1 ± 7	JURASSIC	Silurian		488.5 ± 4.5 491 ± 4	Paleoproterozoic	Paleoproterozoic	2050					
		Lutetian	42.1 ± 1.8	Bajocian	173.5 ± 11.5		EARLY	Ludlovian	424 ± 4								
PALEOGENE	Eocene	Bartonian	38.6 ± 1.5	Aalenian	178 ± 11	TRIASSIC		EARLY	Wentlockian	430.4 ± 9	Neoproterozoic	Neoproterozoic	2300				
		Lutetian	42.1 ± 1.8	Toarcian	187 ± 15		MIDDLE		Llandoveryian	439 ± 7							
	Eocene	Lutetian	42.1 ± 1.8	Pliensbachian	187 ± 15	LATE		Gamachian	(445)								
		Ypresian	50 ± 1.5	Sinemurian	194.5 ± 5		EARLY	Richmondian	(452)								
Eocene	Ypresian	50 ± 1.5	Hettangian	203.5 ± 6.5	ORDOVICIAN	Maysvillian		(458)									
	Thanetian	60.5 ± 2.3	Norian	208 ± 7.5		MIDDLE	Edenian	464 ± 7.5									
Eocene	Thanetian	60.5 ± 2.3	Carnian	225.4 ± 9.5	CAMBRIAN		Tranionian	(467)									
	Danian	65 ± 2	Ladinian	235 ± 4		EARLY	Blackriverian	(470)									
Eocene	Thanetian	60.5 ± 2.3	Spathian	241 ± 8	LATE		Chazyian	(473)									
	Danian	65 ± 2	Dienerian	(242)		MIDDLE	Walterekian	476 ± 7.5									
Eocene	Thanetian	60.5 ± 2.3	Griesbachian	245 ± 9.5	EARLY		Canadian	510 ± 9.5									
	Danian	65 ± 2	Waucoban	536 ± 5.5		LATE	Canadian	510 ± 9.5									
Eocene	Thanetian	60.5 ± 2.3	Waucoban	536 ± 5.5	EARLY		Canadian	510 ± 9.5									
	Danian	65 ± 2	Placentian	(553)		MIDDLE	Canadian	510 ± 9.5									
Eocene	Thanetian	60.5 ± 2.3	Placentian	(553)	EARLY		Canadian	510 ± 9.5									
	Danian	65 ± 2	Placentian	(553)		MIDDLE	Canadian	510 ± 9.5									
Eocene	Thanetian	60.5 ± 2.3	Placentian	(553)	EARLY		Canadian	510 ± 9.5									
	Danian	65 ± 2	Placentian	(553)		MIDDLE	Canadian	510 ± 9.5									
Eocene	Thanetian	60.5 ± 2.3	Placentian	(553)	EARLY		Canadian	510 ± 9.5									
	Danian	65 ± 2	Placentian	(553)		MIDDLE	Canadian	510 ± 9.5									
Eocene	Thanetian	60.5 ± 2.3	Placentian	(553)	EARLY		Canadian	510 ± 9.5									
	Danian	65 ± 2	Placentian	(553)		MIDDLE	Canadian	510 ± 9.5									
Eocene	Thanetian	60.5 ± 2.3	Placentian	(553)	EARLY		Canadian	510 ± 9.5									
	Danian	65 ± 2	Placentian	(553)		MIDDLE	Canadian	510 ± 9.5									
Eocene	Thanetian	60.5 ± 2.3	Placentian	(553)	EARLY		Canadian	510 ± 9.5									
	Danian	65 ± 2	Placentian	(553)		MIDDLE	Canadian	510 ± 9.5									
Eocene	Thanetian	60.5 ± 2.3	Placentian	(553)	EARLY		Canadian	510 ± 9.5									
	Danian	65 ± 2	Placentian	(553)		MIDDLE	Canadian	510 ± 9.5									
Eocene	Thanetian	60.5 ± 2.3	Placentian	(553)	EARLY		Canadian	510 ± 9.5									
	Danian	65 ± 2	Placentian	(553)		MIDDLE	Canadian	510 ± 9.5									
Eocene	Thanetian	60.5 ± 2.3	Placentian	(553)	EARLY		Canadian	510 ± 9.5									
	Danian	65 ± 2	Placentian	(553)		MIDDLE	Canadian	510 ± 9.5									
Eocene	Thanetian	60.5 ± 2.3	Placentian	(553)	EARLY		Canadian	510 ± 9.5									
	Danian	65 ± 2	Placentian	(553)		MIDDLE	Canadian	510 ± 9.5									
Eocene	Thanetian	60.5 ± 2.3	Placentian	(553)	EARLY		Canadian	510 ± 9.5									
	Danian	65 ± 2	Placentian	(553)		MIDDLE	Canadian	510 ± 9.5									
Eocene	Thanetian	60.5 ± 2.3	Placentian	(553)	EARLY		Canadian	510 ± 9.5									
	Danian	65 ± 2	Placentian	(553)		MIDDLE	Canadian	510 ± 9.5									
Eocene	Thanetian	60.5 ± 2.3	Placentian	(553)	EARLY		Canadian	510 ± 9.5									
	Danian	65 ± 2	Placentian	(553)		MIDDLE	Canadian	510 ± 9.5									
Eocene	Thanetian	60.5 ± 2.3	Placentian	(553)	EARLY		Canadian	510 ± 9.5									
	Danian	65 ± 2	Placentian	(553)		MIDDLE	Canadian	510 ± 9.5									
Eocene	Thanetian	60.5 ± 2.3	Placentian	(553)	EARLY		Canadian	510 ± 9.5									
	Danian	65 ± 2	Placentian	(553)		MIDDLE	Canadian	510 ± 9.5									
Eocene	Thanetian	60.5 ± 2.3	Placentian	(553)	EARLY		Canadian	510 ± 9.5									
	Danian	65 ± 2	Placentian	(553)		MIDDLE	Canadian	510 ± 9.5									
Eocene	Thanetian	60.5 ± 2.3	Placentian	(553)	EARLY		Canadian	510 ± 9.5									
	Danian	65 ± 2	Placentian	(553)		MIDDLE	Canadian	510 ± 9.5									
Eocene	Thanetian	60.5 ± 2.3	Placentian	(553)	EARLY		Canadian	510 ± 9.5									
	Danian	65 ± 2	Placentian	(553)		MIDDLE	Canadian	510 ± 9.5									
Eocene	Thanetian	60.5 ± 2.3	Placentian	(553)	EARLY		Canadian	510 ± 9.5									
	Danian	65 ± 2	Placentian	(553)		MIDDLE	Canadian	510 ± 9.5									
Eocene	Thanetian	60.5 ± 2.3	Placentian	(553)	EARLY		Canadian	510 ± 9.5									
	Danian	65 ± 2	Placentian	(553)		MIDDLE	Canadian	510 ± 9.5									
Eocene	Thanetian	60.5 ± 2.3	Placentian	(553)	EARLY		Canadian	510 ± 9.5									
	Danian	65 ± 2	Placentian	(553)		MIDDLE	Canadian	510 ± 9.5									
Eocene	Thanetian	60.5 ± 2.3	Placentian	(553)	EARLY		Canadian	510 ± 9.5									
	Danian	65 ± 2	Placentian	(553)		MIDDLE	Canadian	510 ± 9.5									
Eocene	Thanetian	60.5 ± 2.3	Placentian	(553)	EARLY		Canadian	510 ± 9.5									
	Danian	65 ± 2	Placentian	(553)		MIDDLE	Canadian	510 ± 9.5									
Eocene	Thanetian	60.5 ± 2.3	Placentian	(553)	EARLY		Canadian	510 ± 9.5									
	Danian	65 ± 2	Placentian	(553)		MIDDLE	Canadian	510 ± 9.5									
Eocene	Thanetian	60.5 ± 2.3	Placentian	(553)	EARLY		Canadian	510 ± 9.5									
	Danian	65 ± 2	Placentian	(553)		MIDDLE	Canadian	510 ± 9.5									
Eocene	Thanetian	60.5 ± 2.3	Placentian	(553)	EARLY		Canadian	510 ± 9.5									
	Danian	65 ± 2	Placentian	(553)		MIDDLE	Canadian	510 ± 9.5									
Eocene	Thanetian	60.5 ± 2.3	Placentian	(553)	EARLY		Canadian	510 ± 9.5									
	Danian	65 ± 2	Placentian	(553)		MIDDLE	Canadian	510 ± 9.5									
Eocene	Thanetian	60.5 ± 2.3	Placentian	(553)	EARLY		Canadian	510 ± 9.5									
	Danian	65 ± 2	Placentian	(553)		MIDDLE	Canadian	510 ± 9.5									
Eocene	Thanetian	60.5 ± 2.3	Placentian	(553)	EARLY		Canadian	510 ± 9.5									
	Danian	65 ± 2	Placentian	(553)		MIDDLE	Canadian	510 ± 9.5									
Eocene	Thanetian	60.5 ± 2.3	Placentian	(553)	EARLY		Canadian	510 ± 9.5									
	Danian	65 ± 2	Placentian	(553)		MIDDLE	Canadian	510 ± 9.5									
Eocene	Thanetian	60.5 ± 2.3	Placentian	(553)	EARLY		Canadian	510 ± 9.5									
	Danian	65 ± 2	Placentian	(553)		MIDDLE	Canadian	510 ± 9.5									
Eocene	Thanetian	60.5 ± 2.3	Placentian	(553)	EARLY		Canadian	510 ± 9.5									
	Danian	65 ± 2	Placentian	(553)		MIDDLE	Canadian	510 ± 9.5									
Eocene	Thanetian	60.5 ± 2.3	Placentian	(553)	EARLY		Canadian	510 ± 9.5									
	Danian	65 ± 2	Placentian	(553)		MIDDLE	Canadian	510 ± 9.5									
Eocene	Thanetian	60.5 ± 2.3	Placentian	(553)	EARLY		Canadian	510 ± 9.5									
	Danian	65 ± 2	Placentian	(553)		MIDDLE	Canadian	510 ± 9.5									
Eocene	Thanetian	60.5 ± 2.3	Placentian	(553)	EARLY		Canadian	510 ± 9.5									
	Danian	65 ± 2	Placentian	(553)		MIDDLE	Canadian	510 ± 9.5									
Eocene	Thanetian	60.5 ± 2.3	Placentian	(553)	EARLY		Canadian	510 ± 9.5									
	Danian	65 ± 2	Placentian	(553)		MIDDLE	Canadian	510 ± 9.5									
Eocene	Thanetian	60.5 ± 2.3	Placentian	(553)	EARLY		Canadian	510 ± 9.5									
	Danian	65 ± 2	Placentian	(553)		MIDDLE	Canadian	510 ± 9.5									
Eocene	Thanetian	60.5 ± 2.3	Placentian	(553)	EARLY		Canadian	510 ± 9.5									
	Danian	65 ± 2	Placentian	(553)		MIDDLE	Canadian	510 ± 9.5									
Eocene	Thanetian	60.5 ± 2.3	Placentian	(553)	EARLY		Canadian	510 ± 9.5									
	Danian	65 ± 2	Placentian	(553)		MIDDLE	Canadian	510 ± 9.5									
Eocene	Thanetian	60.5 ± 2.3	Placentian	(553)	EARLY		Canadian	510 ± 9.5									
	Danian	65 ± 2	Placentian	(553)		MIDDLE	Canadian	510 ± 9.5									
Eocene	Thanetian	60.5 ± 2.3	Placentian	(553)	EARLY		Canadian	510 ± 9.5									
	Danian	65 ± 2	Placentian	(553)		MIDDLE	Canadian	510 ± 9.5									
Eocene	Thanetian	60.5 ± 2.3	Placentian	(553)	EARLY		Canadian	510 ± 9.5									
	Danian	65 ± 2	Placentian	(553)		MIDDLE	Canadian	510 ± 9.5									
Eocene	Thanetian	60.5 ± 2.3	Placentian	(553)	EARLY		Canadian	510 ± 9.5									
	Danian	65 ± 2	Placentian	(553)		MIDDLE	Canadian	510 ± 9.5									
Eocene	Thanetian	60.5 ± 2.3	Placentian	(553)	EARLY		Canadian	510 ± 9.5									
	Danian	65 ± 2	Placentian	(553)		MIDDLE	Canadian	510 ± 9.5									
Eocene	Thanetian	60.5 ± 2.3	Placentian	(553)	EARLY		Canadian	510 ± 9.5									
	Danian	65 ± 2	Placentian	(553)		MIDDLE	Canadian	510 ± 9.5									
Eocene	Thanetian	60.5 ± 2.3	Placentian	(553)	EARLY		Canadian	510 ± 9.5									
	Danian	65 ± 2	Placentian	(553)		MIDDLE	Canadian	510 ± 9.5									
Eocene	Thanetian	60.5 ± 2.3	Placentian	(553)	EARLY		Canadian	510 ± 9.5									
	Danian	65 ± 2	Placentian	(553)		MIDDLE	Canadian	510 ± 9.5									
Eocene	Thanetian	60.5 ± 2.3	Placentian	(553)	EARLY		Canadian	510 ± 9.5									
	Danian	65 ± 2	Placentian	(553)		MIDDLE	Canadian	510 ± 9.5									
Eocene	Thanetian	60.5 ± 2.3	Placentian	(553)	EARLY		Canadian	510 ± 9.5									
	Danian	65 ± 2	Placentian	(553)		MIDDLE	Canadian	510 ± 9.5									
Eocene	Thanetian	60.5 ± 2.3	Placentian	(553)	EARLY		Canadian	510 ± 9.5									
	Danian	65 ± 2	Placentian	(553)		MIDDLE	Canadian	510 ± 9.5									
Eocene	Thanetian	60.5 ± 2.3	Placentian	(553)	EARLY		Canadian	510 ± 9.5									
	Danian	65 ± 2	Placentian	(553													